
Manfried Faber



TECHNISCHE
UNIVERSITÄT
WIEN
Vienna University of Technology

DIPLOMARBEIT

Charged particles in the model of topological fermions

ausgeführt am
Atominstitut
der Technischen Universität Wien

unter der Anleitung von

Ao. Univ. Prof. i. R. Dipl.-Ing. Dr. techn. Manfred Faber

durch

Dominik Theuerkauf
Castellezgasse 2/18
A-1020 Wien

Wien, 5. Mai 2016

Dominik Theuerkauf

Abstract

The *model of topological fermions* describes particles with spin quantum number $1/2$ as solutions of a nonlinear partial differential equation. Single particle solutions are stable and characterised by topological quantum numbers, they are topological *solitons*. For introducing the concept the soliton solutions of the $1+1$ dimensional sine-Gordon equation are presented first. Then we define the model in $3+1$ dimensions and describe charged particles. We sketch the mathematic toolkit – Lie groups and Lie algebras, using quaternions for visualizing the necessary considerations. Field and energy density of single solitons is calculated and the relation of the curvature in color space to the electric field in real space will be explained. In addition, two topological quantum numbers are introduced, characterizing spin and charge of topological fermions. The soliton fields are interpreted as extended objects in real space – the topological fermions, compared to the first generation of leptons (e^- , e^+). It is shown that far away from the soliton centers – in the *electrodynamic limit* – the electromagnetic interaction behaves like the Coulomb interaction.

In the second part, we investigate a quasi static collision of two topological fermions by calculating the total energy of soliton fields with decreasing distance on a lattice. For this purpose, we have programmed a computer simulation. Due to size and runtime limits of the discrete lattice simulation, an additional surface energy term has to be included. This surface term is evaluated in the electrodynamic limit. To stabilize the lattice solutions, we freeze the values of the soliton-field around the soliton centers and the field at the boundaries of the lattice, initialized by precalculated values of the electric field of a normal dipole from Maxwell's theory. Comparing the lattice simulation of a single soliton with the algebraic solutions, we find an error of less than $1/2\%$.

However, the more interesting part is the comparison of the interaction of the two soliton with the calculated total energy of a particle-antiparticle¹ dipole. At distances of the soliton center smaller than $10r_0$ with r_0 denoting the soliton radius the interaction starts to deviate from Coulomb's $1/r^2$ -law. This behaviour, which is also known from QED, can be interpreted as *running*

¹For better comparability we have effectively used the values of an electron-positron dipole.

II

coupling.

Contents

1	Introduction	3
1.1	Historical digest	3
1.1.1	Fermions and bosons	4
1.1.2	Solitons	5
1.2	The Sine-Gordon model	5
2	Structure and geometry	8
2.1	Abstract group definition	8
2.2	Vector space	9
2.3	General linear groups	10
2.3.1	Subgroups	10
2.3.2	Rotational group $\mathbf{SO}(3)$, complex group $\mathbf{SU}(2)$	11
2.3.3	Linear Lie-groups and tangent space	12
2.4	Lie-algebra	13
2.4.1	Representation of Lie-algebras	14
2.4.2	Special unitary Lie-algebra $\mathfrak{su}(n)$	15
2.5	Quaternions	16
2.5.1	Norm and conjugation	17
2.5.2	Rotations	18
2.5.3	Derivative	21
2.5.4	Curvature	23
3	Model of topological fermions	25
3.1	Hedgehog approach	26
3.1.1	Affine connection	27
3.2	Lagrangian density	28
3.2.1	Solution of soliton monopole	30
3.3	Stable soliton configuration	31
3.4	Dipole soliton configuration	34
3.4.1	Electric field of a dipole	37
3.4.2	Cylindrical symmetric configuration	38

4	Lattice computation	41
4.1	Evaluating total energy	42
4.1.1	Summation of total energy	43
4.1.2	Energy contribution of a monopole outside the box . . .	44
4.1.3	<i>Hartree</i> atomic units	46
4.1.4	Energy Contribution of a dipole outside the box	47
4.2	Computation of action	48
4.2.1	Gauge fields and Wilson action	49
5	Results	53
5.1	Using Computer program <code>sol</code>	53
5.2	Accuracy	55
5.2.1	Boundary conditions	56
5.3	Dipole results	58
5.4	Conclusion	62
A	Equation of motion	64
B	Electric field of a dipole	66
C	Parallel transport and covariant derivative	68
D	Command-line options of program <code>sol</code>	71

Chapter 1

Introduction

Starting with a short overview of the today commonly used *standard model* of interactions and matter, the present physical description is based on a perception of *wave-particle duality* in nature. Since the development of quantum mechanics in the 1920s- and 1930s by the nowadays famous theorists like PLANCK, BOHR, SCHRÖDINGER and later DIRAC et al. until the modern interpretation and calculations of QED, QCD, combined in the *Standard Model*, it is shown in various experiments that elementary particles can be divided into *fermions* and *bosons*.

1.1 Historical digest

First ideas of describing matter by indivisible particles go back to DEMOKRITUS [1] about 400 years B.C. Due to his thoughts and philosophy he named indestructible pieces of matter – so tiny that they become invisible to the human eye – *atoms*. At least 2000 years later, ISAAC NEWTON has tried to describe the nature of light by particles named photons. But his particle model of light is not able to explain diffraction and scattering of light, as does the model of light waves suggested by CHRISTIAN HUYGENS.

In the late 18th century scientists like ANTOINE LAVOISIER, JOHN DALTON and AMEDEO AVOGADRO [2, 3], based on the philosophy of DEMOKRITUS developed an advanced, but similar theory of atomic spheres imagined as tiny hard balls during their chemical experiments. The idea rests upon *Dalton's law of multiple proportions* and is today one of the basic laws of stoichiometry.

In the end of the 19th century LUDWIG BOLTZMANN used the atomic hypothesis for his theoretical work to derive *statistical mechanics* and thus revolutionizing thermodynamics. He explains macroscopic thermodynamic properties of a statistical ensemble of molecules or atoms by calculating the associated *partition function*. JOSEPH JOHN THOMSON discovered in 1879 the first type of fundamental particles – *electrons* – by experiments with cathode ray tubes and could demonstrate their negative electrical charge. In 1908

HANS GEIGER, ERNEST MARSDEN and ERNEST RUTHERFORD have proven the existence of charged and local concentrated cores of atomic particles by their scattering experiments with α -particles on ^{197}Au -foils [4].

On the other hand since JAMES CLERK MAXWELL introduced the concept of fields as well as the Maxwell equations describing the dynamics of electric and magnetic fields. This has been the first field theory, combining electromagnetic and optical phenomena. Also, this first field theory provides an additional important support, regarding light particles (photons) as electromagnetic waves.¹ These waves, being oscillations of the electromagnetic field, propagate with constant speed c in all inertial frames.

1.1.1 Fermions and bosons

In 1906, MAX PLANCK found the law of *black body radiation* by introducing small units of action and multiplicities – the *quanta*. Since then the perception of a microscopic-granular world in the sense of JOHN DALTON’s atomic hypothesis becomes more and more popular. However, *Quantum Mechanics*, which was developed by physicists like ERWIN SCHRÖDINGER, WERNER HEISENBERG, NIELS BOHR et. al., describes particles and radiation in a dual formalism – *wave-particle duality* – and triggers the modern interpretation of elementary particles.

A lot of different particles² were found in various experiments in the 50th and 60th of the last century. Despite of measurements of different properties of these particles a common classification is used in mathematical manner by an abstract observable called the *spin*. This observable divides particles into two classes:

- *bosons* with integer spin quantum numbers ($s = 0, \pm 1, \dots$) describing the quanta of interactions
- *fermions* with half integer spin quantum numbers ($s = \pm \frac{1}{2}, \pm \frac{3}{2} \dots$) used for matter particles

Modern particle physics is based on *electroweak theory*, a unification of *quantum electrodynamics* (QED) and weak interaction theory and *quantum chromodynamics* (QCD), the theory of *strong interaction*. They are unified in the *Standard model* (SM) [5] of particle physics.

The predictions of the SM are very accurate and reduce the particle zoo to combinations of the fundamental *fermions*, quarks and leptons, and their force carriers – *bosons*. Tab. 1.1 lists the fundamental particles. Despite of the

¹The existence of electromagnetic waves and their propagation with the speed of light has been experimentally proved by HEINRICH HERTZ in the years 1886 - 1889. Nowadays, the speed of light is defined as an explicit constant, $c = 299\,792\,458$ m/s.

²often denoted *particle’s zoo*.

fermions				
leptons			quarks	
1.	electron	e^-	up	u
	electron neutrino	ν_e	down	d
2.	muon	μ^-	charm	c
	muon neutrino	ν_μ	strange	s
3.	tauon	τ^-	top	t
	tauon neutrino	ν_τ	bottom	b
bosons				
electromagnetic interaction			photon	
weak interaction			W^+, W^-, Z^0 bosons	
strong interaction			8 gluons	
gravitational interaction			graviton	

Table 1.1: Listing of all known fundamental particles, 3 generations of leptons, 3 generations of quarks and 12 gauge bosons mediating the 3 fundamental interactions. Only the gravitational force is not yet included in the *standard model*.

graviton³ all predicted fundamental particles have been proved in experiments till today.

1.1.2 Solitons

Solitons are wave phenomena, first mentioned by JOHN SCOTT RUSSEL in 1834. He observed a solitary wave, excited by a braking ship in a channel. That wave run several miles through a channel without modification of its shape. The theoretical explanation was found by DIEDERIK KORTEWEG and GUSTAV DE VRIES in 1895. They investigated a nonlinear partial differential equation of third order, obtaining solutions of the type of Russel's solitary waves. In general, every nonlinear differential equation may have solitary wave solutions.

1.2 The Sine-Gordon model

In nonlinear field theories it is often possible to find solitons as solutions of the differential equations of motion. One of the simplest models to study is the 1+1 dimensional *Sine-Gordon* model. It depends on the solutions of the *Sine-Gordon* equation which is a modification of the *Klein-Gordon* equation. It is a nonlinear hyperbolic partial differential equation which was already considered in the 19th century during the investigation of surfaces of constant Gaussian

³The existence is assumed, not found in experiments, yet.

curvature. About 1962 TONY SKYRME has found that these solutions are able to describe topological solitons which have certain properties of particles [6, 7].

In a mechanical model [8] we couple an ensemble of oscillators along a joint rotation axis with a moment of inertia Θ of each oscillator and torque constant K of the coupling springs in between. One gets

$$\Theta \frac{d^2 \phi_j}{dt^2} = K [\phi_{j+1} - 2\phi_j + \phi_{j-1}] - N \sin \phi_j, \quad (1.1)$$

where $\phi_j = \phi_j(t)$ marks the time dependent amplitude of the j^{th} oscillator and $N \sin \phi_j$ is the gravitational restoring torque. For small amplitudes of ϕ_j we are able to linearize Eq. (1.1) that means $\sin \phi_j \approx \phi_j$ and with $\omega_0^2 = \frac{N}{\Theta}$ we regain the well known Klein-Gordon equation

$$\frac{d^2 \phi_j}{dt^2} + \omega_0^2 \phi_j = \frac{K}{\Theta} [\phi_{j+1} - 2\phi_j + \phi_{j-1}], \quad (1.2)$$

discretised in the space coordinates.

However, considering the long wavelength limit, we assume that the variation of the amplitude of the j^{th} oscillator $\Delta \phi_j = \phi_j - \phi_{j+1}$ is so small that we can replace the difference part $\phi_{j+1} - 2\phi_j + \phi_{j-1}$ by a smooth derivative of the coordinate x . That implies to replace the discrete values ϕ_j by a continuous function of $\phi(x)$. Further we assume an infinite length of the chain. In this approximation we get with $\phi = \phi(x, t)$ and

$$\phi_{j+1} - 2\phi_j + \phi_{j-1} \approx (\Delta x)^2 \frac{\partial^2 \phi}{\partial x^2}$$

the *Sine-Gordon* equation. Furthermore if we measure distance in units of $\sqrt{\frac{K(\Delta x)^2}{N}}$ and time in units of $\sqrt{\frac{\Theta}{N}}$ we will write Eq. (1.1) in compact form

$$\frac{\partial^2 \phi}{\partial x^2} - \frac{\partial^2 \phi}{\partial t^2} = \sin \phi. \quad (1.3)$$

Soliton solutions have the form $\phi(x, t) = \phi(x - vt) = \phi(\xi)$ where v is some velocity of propagation. Using this reduced dependence, Eq. (1.3) can be solved. It reads

$$\phi(x - vt) = 4 \arctan \left[e^{\pm \gamma(\xi - \xi_0)} \right] \quad (1.4)$$

where $\gamma^2 = \frac{1}{1 - \beta^2}$ and $\beta = \frac{v}{v_0}$. This solution describes a one-time twist of the continuous pendulum chain at position ξ_0 . The \pm sign determines a clockwise or anticlockwise rotation and it is named a *kink* and accordingly *anti-kink* solution of Eq. (1.3) (see Fig. 1.1). The kink-anti kink solution are able to travel along their rotational axis with velocity v . They do not change their shape, nor dissipate energy. If two solitons with same (anti-)clockwise rotation crush into each other they do not penetrate, they repel each other. Solitons with

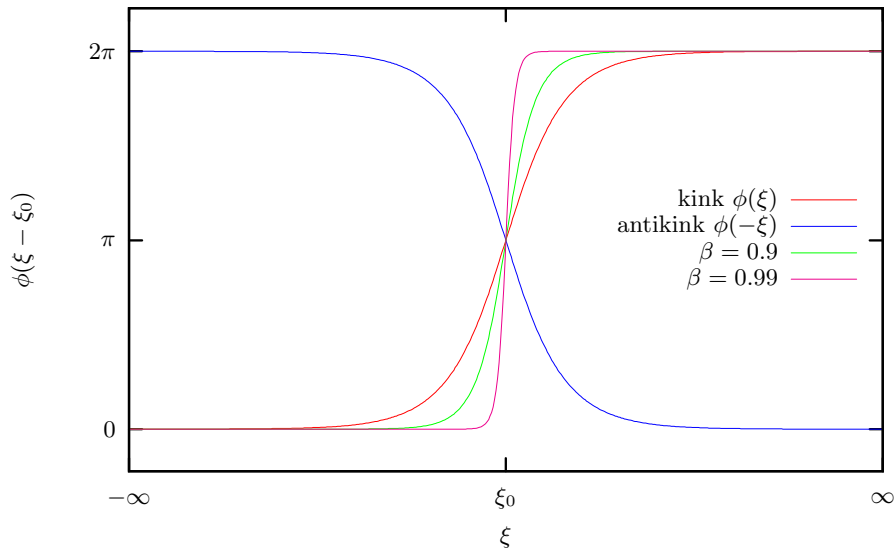


Figure 1.1: Plots of kink- (red) and anti kink-solutions (blue) for the asymptotic values $\phi(\pm\infty) \in \{0, 2\pi\}$. The green and magenta lines show Lorentz contracted kinks for β close to 1. Such kinks are Lorentz contracted.

different helicity annihilate and the energy propagates by small oscillations in both directions.

Static solitons have a given size. Moving solitons show relativistic behaviour. With increasing velocity solitons shrink. In the mechanical model the number of displaced pendulums decreases and the curvature rises.

All these properties demonstrate, kink-anti kink solutions behave similar to particle-antiparticle systems already at the classical level.

Chapter 2

Structure and geometry

In theoretical physics and mathematics continuous symmetries and especially *Lie-groups* are very important subjects. These are based on differentiable manifolds and group operations compatible to their smooth structure. *Lie-groups* are named after SOPHOS LIE (1842 – 1899) a Norwegian mathematician, who developed continuous transformation groups to study symmetries in geometry and in differential equations.

2.1 Abstract group definition

A set \mathbb{G} of elements $g \in \mathbb{G}$ is called an *abstract group* \mathcal{G} with an operation \circ , being the *group law* of \mathcal{G} . To qualify as an *abstract group* $\mathcal{G} = (\mathbb{G}; \circ)$, it has to satisfy four group axioms

- *closure*: For each element a operating on an element b is resulting in exact element $c \in \mathbb{G}$

$$c = a \circ b, \quad \forall a, b, c \in \mathbb{G}. \quad (2.1)$$

- *associativity*: For all elements $a, b, c \in \mathbb{G}$, it is necessary

$$(a \circ b) \circ c = a \circ (b \circ c), \quad \forall a, b, c \in \mathbb{G}. \quad (2.2)$$

- *identity element*: There must exist an *identity element* $e \in \mathbb{G}$ which holds

$$e \circ a = a \circ e = a, \quad \forall a \in \mathbb{G}. \quad (2.3)$$

The *identity element* e is a unique representative in set \mathbb{G} .

- *inverse element*: For an element $a \in \mathbb{G}$ there exists an *inverse element* $b \in \mathbb{G}$ which achieves

$$b \circ a = a \circ b = e, \quad \forall a, b, e \in \mathbb{G}. \quad (2.4)$$

There is an often used notation for $b = a^{-1}$ and $a \circ a^{-1} = e$.

An *abstract group* \mathbb{G} is named a *commutative group* or *Abelian group* if there exists the commutativity axiom

- *commutativity*: For all elements $a, b \in \mathbb{G}$, there is

$$a \circ b = b \circ a, \quad \forall a, b \in \mathbb{G}. \quad (2.5)$$

2.2 Vector space

A set of abstract objects with an operation "+", which forms an Abelian group and may be multiplied by numbers¹, is denoted as *vector space* or *linear space*. In terms of abstract algebra *vector space* has got an *F-module structure*. Besides the axioms of section 2.1, there have to be defined the following additional axioms

- *closure* referring to multiplications of scalars: For all elements \vec{v} of abstract vector space \mathcal{V} and for all scalars $a \in \mathbb{C}$ the result has to be an element of vector space \mathcal{V} .

$$\forall \vec{v} \in \mathcal{V}, \forall a \in \mathbb{C} \quad \text{there must be} \quad a\vec{v} \in \mathcal{V} \quad (2.6)$$

- *distributivity* (or *linearity*): $\forall \vec{v}, \vec{w} \in \mathcal{V}$ and $\forall a, b \in \mathbb{C}$, there exists

$$(a + b)\vec{v} = a\vec{v} + b\vec{v}, \quad (2.7)$$

$$a(\vec{v} + \vec{w}) = a\vec{v} + a\vec{w}, \quad (2.8)$$

$$(ab)\vec{v} = a(b\vec{v}). \quad (2.9)$$

The elements \vec{v} of *vector space* \mathcal{V} can be represented by a sequence or tuple of scalars, called coordinates v_i , multiplied by base vectors \vec{e}_i . A basis is a set \mathcal{E} of linearly independent base vectors $\mathcal{E} = \vec{e}_i, i = 1, \dots, n$, that spans the whole space

$$\vec{v} = \sum_{i=1}^n v_i \vec{e}_i. \quad (2.10)$$

A set \mathbb{S} of n vectors $\vec{s}_i \in \mathbb{S}, i = 1, \dots, n$ is said *linearly independent*, only if all factors a_i vanish and satisfy

$$\vec{0} = \sum_{i=1}^n a_i \vec{v}^i, \quad \forall a_i = 0. \quad (2.11)$$

The dimension of such a set is $\dim \mathbb{S} = n$.

¹This can be regarded as scaling — multiplied by scalar

2.3 General linear groups

An application of the previous structure definitions is the set of invertible $n \times n$ -matrices A_{ij} with $n \in \mathbb{N}$ and $\det A_{ij} \neq 0$. Together with an operation of ordinary matrix multiplication it forms an abstract group. These sets of invertible $n \times n$ -matrices with objects $a_{ij} \in \mathbb{R}$ or $a_{ij} \in \mathbb{C}$ are denoted as *general linear groups*, short $\mathbf{GL}(n, \mathbb{R})$ or $\mathbf{GL}_n(\mathbb{C})$.

All axioms (equations (2.1) – (2.4)) of the abstract group definition in section 2.1 are satisfied, regarding the identity-matrix $\mathbb{1}_n = \delta_{ij}$ as *identity element*. Similarly, the closure is given by the fact that the product of two arbitrary invertible matrices just as well creates an invertible matrix, based on

$$\det(A_{ij}B_{ij}) = \det A_{ij} \det B_{ij} . \quad (2.12)$$

The associativity is inherent to ordinary matrix multiplication, as well as an inverse element A_{ij}^{-1} of each matrix exists due to

$$\det A_{ij} \neq 0 . \quad (2.13)$$

2.3.1 Subgroups

The orthogonal group of dimension n is denoted $\mathbf{O}(n, \mathbb{R})$, or $\mathbf{O}(n)$. It is the group of distance-preserving transformations in *Euclidean space* \mathbb{E}_n with determinant $\det A_{ij} = \pm 1$. The elements of an orthogonal group preserve a non-degenerating symmetric bilinear form on a vector space over real numbers \mathbb{R} [9]. That means it is a set of $n \times n$ -orthogonal matrices with entries of \mathbb{R} , whose transposed elements are equal inverse

$$\mathbf{O}(n) = \left\{ Q \in \mathbf{GL}(n, \mathbb{R}) \mid Q^T Q = Q Q^T = \mathbb{1}_n \right\} . \quad (2.14)$$

Subsequently, the special subgroups $\mathbf{SO}_n(\mathbb{R})$ are the group of orthogonal rotations² with $\det A_{ij} = +1$. In short notation these subgroups are simply written as $\mathbf{SO}(n)$.

The *general unitary group* $\mathbf{U}(n, \mathbb{C})$ is an abstract group of all $n \times n$ -unitary matrices A_{ij} with the group operation of matrix multiplication. It is a subgroup of $\mathbf{GL}(n, \mathbb{C})$ and is a real *Lie*-group of dimension n^2 . In special case of $n = 1$, $\mathbf{U}(1)$, this group corresponds to the *circle group* consisting of all complex numbers $z = e^{i\theta}$ with norm $\|z\| = \sqrt{zz^*} = 1$. There is also a group homomorphism between $\mathbf{U}(n)$ and $\mathbf{U}(1)$ by calculating the determinant

$$\det : \mathbf{U}(n) \longmapsto \mathbf{U}(1) \quad (2.15)$$

²This name is widely used in context of $\mathbf{SO}(2)$, $\mathbf{SO}(3)$, whose elements are the usual rotations around a point in 2-dim space and around a line in 3-dim space.

Group \mathcal{G}	$n \times n$ -Matrix $A \in \mathcal{G}$	$\dim \mathcal{G}$
general linear $\mathbf{GL}(n, \mathbb{R})$	$A_{ij} \in \mathbb{R}, \det A \neq 0$	n^2
$\mathbf{GL}(n, \mathbb{C})$	$A_{ij} \in \mathbb{C}, \det A \neq 0$	$2n^2$
special linear $\mathbf{SL}(n, \mathbb{R})$	$A \in \mathbf{GL}(n, \mathbb{R}), \det A = 1$	$n^2 - 1$
$\mathbf{SL}(n, \mathbb{C})$	$A \in \mathbf{GL}(n, \mathbb{C}), \det A = 1$	$2(n^2 - 1)$
orthogonal $\mathbf{O}(n, \mathbb{R}), \mathbf{O}(n)$	$A \in \mathbf{GL}(n, \mathbb{R}), AA^T = \mathbb{1}_n, \det A = \pm 1$	$n(n-1)/2$
$\mathbf{O}(n, \mathbb{C})$	$A \in \mathbf{GL}(n, \mathbb{C}), AA^T = \mathbb{1}_n, \det A = \pm 1$	$n(n-1)$
special orthogonal $\mathbf{SO}(n, \mathbb{R}), \mathbf{SO}(n)$	$A \in \mathbf{O}(n), \det A = 1$	$n(n-1)/2$
$\mathbf{SO}(n, \mathbb{C})$	$A \in \mathbf{O}(n, \mathbb{C}), \det A = 1$	$n(n-1)$
unitary $\mathbf{U}(n)$	$A \in \mathbf{GL}(n, \mathbb{C}), AA^\dagger = \mathbb{1}_n, \det A = 1$	n^2
special unitary $\mathbf{SU}(n)$	$A \in \mathbf{U}(n), \det A = 1$	$n^2 - 1$

Table 2.1: Summary of several subgroups in n dimensions of $\mathbf{GL}(n, \mathbb{K})$ as submanifolds of \mathbb{R}^{n^2} , if $\mathbb{K} = \mathbb{R}$ or \mathbb{R}^{2n^2} , if $\mathbb{K} = \mathbb{C}$. (Excerpt from page 148 of [10].)

The kernel of this group homomorphism is the set of $n \times n$ -unitary matrices with determinant $\det U_{ij} = 1$. Hence, $\mathbf{U}(n)$ may be written as semidirect product $\mathbf{U}(n) = \mathbf{SU}(n) \times \mathbf{U}(1)$.

Subsequently, the special subgroups $\mathbf{SU}(n, \mathbb{C})$ or $\mathbf{SU}(n)$ are the set of $n \times n$ -unitary matrices with determinant $\det U_{ij} = 1$. In modern particle physics they are very important ³.

2.3.2 Rotational group $\mathbf{SO}(3)$, complex group $\mathbf{SU}(2)$

In geometry the group of all rotations in Euclidean space \mathbb{E}_3 under the operation of composition is denoted rotational group, see section 2.3.1. Rotations are linear transformations of \mathbb{R}^3 and therefore preserving length and angles of vectors, which is equivalent to preserving the inner – the dot product of vectors.

For any element $D(\omega) \in \mathbf{SO}(3)$ with rotational angle $\omega \in \mathbb{R}$, the scalar product of two vectors $\vec{r}, \vec{s} \in \mathcal{V} \subseteq \mathbb{R}^3$ has to be preserved.

$$\begin{aligned} \vec{r}' &= D(\omega)\vec{r}, \\ \vec{s}' &= D(\omega)\vec{s}. \end{aligned} \tag{2.16}$$

³ $\mathbf{SU}(2)$ is used to describe the spin, further it is important for electroweak interactions. The colour group $\mathbf{SU}(3)$ turned out to be substantial for quantum chromodynamics [5].

The scalar product in index-notation⁴ is

$$r_i s_i = r'_i s'_i = D_{ij} r_j D_{ik} s_k = r_j D_{ji}^T D_{ik} s_k . \quad (2.17)$$

Therefore the following constraint is required

$$D_{ji}^T D_{ik} = \delta_{jk} . \quad (2.18)$$

Orthogonal matrices D_{ij} with the $\det[D(\omega)] = +1$ are elements of the group $\mathbf{SO}(3)$. The determinant (+1) ensures the chirality and the orthonormalization of the rotated vectors.

The special unitary group $\mathbf{SU}(2)$ comprises the complex rotations in two-dimensional complex space \mathbb{C}^2 and the group elements $U \in \mathbf{SU}(2)$ fulfill the following properties

$$\begin{aligned} U^\dagger U &= \mathbb{1}_2 , \\ \det U &= 1 . \end{aligned} \quad (2.19)$$

The group $\mathbf{SU}(2)$ is isomorphic⁵ to the group \mathcal{H}_{unit} , which consists of the set \mathbb{H}_{unit} , the set of unit quaternions⁶ and the quaternion multiplication as group operation. Besides, the group $\mathbf{SU}(2)$ is diffeomorphic⁷ to the unit sphere \mathbb{S}^3 . Since unit quaternions are used to represent rotations in 3-dimensional space \mathbb{E}_3 there is an *epimorphism* from $\mathbf{SU}(2)$ to the rotational group $\mathbf{SO}(3)$.

2.3.3 Linear Lie-groups and tangent space

The definition of *Lie-groups* is based on $n \times n$ -matrices with the above mentioned properties. There are uncountably infinite elements in *Lie-groups*,

⁴and also using *Einstein summation convention*

⁵group-*homomorphism* is a mapping ψ of a group \mathcal{G} with an operation \circ to a group \mathcal{G}' with operation $*$

$$\psi : \mathcal{G} \mapsto \mathcal{G}'$$

where ψ preserves the structure of operations

$$\psi(g \circ h) = \psi(g) * \psi(h) \quad \forall g, h \in \mathcal{G} .$$

Hence, the mapping of an operation $a \circ b$ is equal to the mapping $\psi(a)$ linked to the mapping $\psi(b)$. In the case of an injective mapping it is denoted *monomorphism*, a surjective mapping is denoted *epimorphism*.

If the homomorphic mapping is injective and surjective, in short term bijective it is called *isomorphism*. Both groups \mathcal{G} and \mathcal{G}' are equivalent.

$$\psi : \mathcal{G} \mapsto \mathcal{G}' \quad \mathcal{G} \cong \mathcal{G}'$$

An *automorphism* is an isomorphic mapping ψ with identical structures $\{\mathcal{G}, \circ\}$ and $\{\mathcal{G}', *\}$.

⁶The abstract group \mathcal{H}_{unit} is defined

$$\mathcal{H}_{unit} = (\mathbb{H}_{unit}; \odot) \quad \text{with} \quad \mathbb{H}_{unit} \subseteq \mathbb{H} .$$

In section 2.5 on page 16 the sets \mathbb{H} and \mathbb{H}_{unit} are described in detail.

⁷A mapping Φ is denoted *diffeomorphic*, if there exists an invertible mapping Φ^{-1} and if Φ and Φ^{-1} are differentiable.

which form topology spaces and inherit the properties of topological groups. In addition, they also form an analytic manifold with mappings to itself as group operation [10]. Particularly interesting in a physical manner are the *linear Lie-groups* being represented by finite dimensional matrices for their application in describing fundamental interactions [5].

Because of the homogeneity of these topological groups it is sufficient to examine their structure near the identity element $\mathbb{1}_n$. However, nearness and vicinity of group elements forces to establish a metric. The *tangent space* \mathcal{T} of such a group element is a linear vector space. Establishing a distance function in this group, enables to view it as euclidean space with dimension n . Similar to the well known euclidean vector space, we define a scalar product of two group elements

$$A \cdot B = \frac{1}{n} \sum_{ij=1}^n (A_{ij} B_{ij}) = \frac{1}{n} \text{Tr} [A^T B] \quad (2.20)$$

and a distance function d with the following properties:

$$d(q, q') = d(q', q) \quad \forall q, q' \in \mathcal{G} \quad \text{symmetry}, \quad (2.21)$$

$$d(q, q') = 0 \quad \text{only if } q = q', \quad (2.22)$$

$$d(q, q') > 0 \quad \text{if } q \neq q', \quad (2.23)$$

$$d(q, q') \leq d(q, q'') + d(q'', q') \quad \forall q, q', q'' \in \mathcal{G} \quad \text{triangle inequality}. \quad (2.24)$$

A metric space is a set of elements of group \mathcal{G} together with a metric on \mathcal{G} . Now we are able to define a metric representation $d(A, B)$ for elements of *general linear groups* and subgroups.

$$\begin{aligned} d(A, B) &= \sqrt{\frac{1}{n} \sum_{ij=1}^n |A_{ij} - B_{ij}|^2} \\ &= \sqrt{\frac{1}{n} \text{Tr} [(A - B)^T (A - B)]}. \end{aligned} \quad (2.25)$$

The norm or absolute value of these elements can be considered as the distance to the n -dimensional zero matrix 0_n

$$\|A\| = d(0_n, A) = \sqrt{\frac{1}{n} \text{Tr} [A^T A]}. \quad (2.26)$$

2.4 Lie-algebra

As mentioned, analyzing *Lie-groups* is based on linearising these groups along the identity element $\mathbb{1}_n$. This reveals the corresponding *Lie-algebra*, showing the local structure of a *Lie-group* around the identity element $\mathbb{1}_n$. That implies a major advance in exploring representations of *Lie-groups*.

A set of elements a, b, c, \dots of the vector space \mathcal{V} over a field \mathbb{K} with $\dim \mathcal{V} = n$ and \mathbb{K} is either \mathbb{R} or \mathbb{C} together with the operator *commutator* $[\cdot, \cdot] : \mathcal{V} \times \mathcal{V} \mapsto \mathcal{V}$, also denoted *Lie-bracket*, is called *Lie-algebra* \mathfrak{gl} , if they satisfy the following axioms

- *closure*: For all elements $a, b \in \mathfrak{gl}$, the result also has to be an element of vector space \mathfrak{gl}

$$[a, b] \in \mathfrak{gl}, \quad \forall a, b \in \mathfrak{gl}. \quad (2.27)$$

- *bilinearity*: $\forall a, b, c \in \mathfrak{gl}$ and $\forall \alpha, \beta \in \mathbb{C}$, there exists

$$[\alpha a + \beta b, c] = \alpha [a, c] + \beta [b, c], \quad (2.28)$$

$$[a, \alpha b + \beta c] = \alpha [a, b] + \beta [a, c]. \quad (2.29)$$

- *alternativity* on \mathfrak{gl}

$$[a, a] = 0, \quad \forall a \in \mathfrak{gl}. \quad (2.30)$$

- *Jacobi identity*

$$[a, [b, c]] = [b, [c, a]] = [c, [a, b]] = 0, \quad \forall a, b, c \in \mathfrak{gl}. \quad (2.31)$$

Considering *bilinearity* (2.28) and *alternativity* (2.31), one obtains *anticommutativity*

$$[a, b] = -[b, a], \quad \forall a, b \in \mathfrak{gl}. \quad (2.32)$$

2.4.1 Representation of Lie-algebras

Each element of a *Lie-group* can be described as

$$U(\phi_k) = e^{-i \sum_{k=1}^n \phi_k T_k} \equiv e^{-i \phi_k T_k} \quad (2.33)$$

with the n group-parameters ϕ_k and the generators T_k of this *Lie-group*. The generators form a n -dimensional *Lie-algebra*. They can be obtained by differentiating an element with respect to the group-parameters

$$\left. \frac{\partial U}{\partial \phi_k} \right|_{\phi_k=0} = -iT_k U \Big|_{\phi_k=0} = -iT_k. \quad (2.34)$$

Hence, the generators create the tangent space at the identity element

$$U(\delta \phi_k) = \mathbb{1}_n - i \delta \phi_k T_k \quad (2.35)$$

and with the related group operation $[\cdot, \cdot]$, the *Lie-bracket*, they satisfy equations (2.27) – (2.31).

$$[T_k, T_l] = T_k T_l - T_l T_k = i f_{kl}^m T_m \quad (2.36)$$

determines the group structure of the *Lie-group*. The *structure constants* f_{kl}^m are total antisymmetric with respect to permutation of indices.

2.4.2 Special unitary Lie-algebra $\mathfrak{su}(n)$

As previously mentioned, the Lie-algebra $\mathfrak{su}(n)$ consists of a set of traceless antihermitian $n \times n$ -matrices with the commutator operation as *Lie-bracket*. Due to the property of traceless matrices, the number of independent generators is $n^2 - 1$. According to [11, 12] the *Lie-algebra* $\mathfrak{su}(n)$ can be constructed by n^2 Operators $\{\hat{N}_{kl} | k, l = 1, \dots, n\}$, which satisfy the following commutation relation:

$$[\hat{N}_{kl}, \hat{N}_{mo}] = \delta_{lm}\hat{N}_{ko} - \delta_{ko}\hat{N}_{ml} \quad (2.37)$$

for $k, l, m, o = 1, \dots, n$. In addition, summing over all traces of operators

$$\hat{M} = \sum_{k=1}^n \hat{N}_{kk}$$

there is

$$[\hat{M}, \hat{N}_{kl}] = 0 \quad (2.38)$$

implying the number of generators of the Lie-algebra decreases to $n^2 - 1$.

Generators in *fundamental* representation $\{T_k | k = 1, \dots, n^2 - 1\}$ generally fulfill

$$T_k T_l = \frac{1}{2n} \delta_{kl} \mathbb{1}_n + \frac{1}{2} \sum_{m=1}^{n^2-1} (i f_{kl}^m + d_{kl}^m) T_m \quad (2.39)$$

with antisymmetric structure constants f_{kl}^m and structure constants d_{kl}^m , which are symmetric in all indices. Hence, the Lie-bracket is divided to a commutator and anticommutator operation

$$[T_k, T_l] = i \sum_{m=1}^{n^2-1} f_{kl}^m T_m, \quad (2.40)$$

$$\{T_k, T_l\} = \frac{1}{n} \delta_{kl} \mathbb{1}_n + \sum_{m=1}^{n^2-1} d_{kl}^m T_m. \quad (2.41)$$

As a normalisation convention for the symmetric structure constants we write

$$\sum_{k,l=1}^{n^2-1} d_{klm} d^{kl}_o = \frac{n^2 - 4}{n} \delta_{mo}. \quad (2.42)$$

As an example let us have a closer look at the Lie-algebra $\mathfrak{su}(2)$. Based on the linear independence of the generators T_k with $\{T_k | k = 1, 2, 3\}$ of the Lie-group $\mathbf{SU}(2)$ over the field \mathbb{C} , one generates the Lie-algebra $\mathfrak{su}(2)$ defining the following commutator relations

$$[T_1, T_2] = iT_3 \quad [T_2, T_3] = iT_1 \quad [T_3, T_1] = iT_2 \quad (2.43)$$

respective

$$[T_i, T_j] = i \sum_{k=1}^3 \varepsilon_{ij}^k T_k \equiv i \varepsilon_{ij}^k T_k \quad (2.44)$$

with total antisymmetric structure constants ε_{ij}^k (*Levi-Civita symbol*).

$$\varepsilon_{ijk} = \varepsilon_{ij}^k = \begin{cases} 1 & \text{if } ijk \text{ is an even permutation} \\ 0 & \text{if } ijk \text{ has equal indices} \\ -1 & \text{if } ijk \text{ is an odd permutation} \end{cases} \quad (2.45)$$

The tensors $\{\varepsilon^k | k = 1, 2, 3\}$ are identical to the generators of the rotational group $\mathbf{SO}(3)$, due to an isomorphism between $\mathfrak{su}(2)$ and $\mathfrak{so}(3)$. These elements $T_k \in \mathfrak{su}(2)$ are linear and antihermitian operators $T_k^\dagger = -T_k$.

Otherwise, using *Pauli spin-matrices*⁸ σ_i , one gets the *fundamental* or *defining* representation of the Lie-algebra $\mathfrak{su}(2)$ by

$$J_k = \frac{\sigma_k}{2} \quad \text{and} \quad [J_i, J_j] = i \varepsilon_{ij}^k J_k. \quad (2.46)$$

These relations define the spin operator \hat{S}_i in quantum mechanics up to a factor of \hbar . The elements $J_k \in \mathfrak{su}(2)$ are hermitian $J_k^\dagger = J_k$ with trace $\text{Tr}[J_k] = 0$ and subsequently the eigenvalues become real [13, 15].

The generators is the $n^2 - 1$ -dimensional *adjoint* representation can be defined using the structure constants f_{klm} . For $n = 2$ they read

$$(T_k)_{lm} = -i f_{klm} = -i \varepsilon_{klm}. \quad (2.47)$$

2.5 Quaternions

In historical context, *quaternions* has been found by BENJAMIN OLINDE RODRIGUES in 1840 and again by WILLIAM ROWAN HAMILTON in 1843. Their motivation was induced by the problem of rotations in 3-dimensional space. Rotations in a 2-dimensional plane can be described with the help of normalised complex numbers. The rotational angle is the corresponding complex number, used as a vector in \mathbb{R}^2 . Consecutively processing of several rotations is calculated by multiplications in the field \mathbb{C} . Generalizing complex numbers *quaternions* are represented as 4-tuples $Q = (q_0, \vec{q}) = (q_0, q_i)$ with $i = 1, 2, 3$. The set of all quaternions is denoted $\mathbb{H} = \{Q | q_0, q_i \in \mathbb{R}, i = 1, 2, 3\}$.

⁸The *Pauli-matrices* are defined by

$$\sigma_1 = \begin{pmatrix} 0 & 1 \\ 1 & 0 \end{pmatrix}, \quad \sigma_2 = \begin{pmatrix} 0 & -i \\ i & 0 \end{pmatrix}, \quad \sigma_3 = \begin{pmatrix} 1 & 0 \\ 0 & -1 \end{pmatrix}.$$

Another equivalent notation is using beside $i = \sqrt{-1}$ further imaginary units j, k . It requires

$$i^2 = j^2 = k^2 = ijk = -1 \quad (2.48)$$

and a quaternion $Q \in \mathbb{H}$ is written in the form

$$Q = q_0 + iq_1 + jq_2 + kq_3 \quad (2.49)$$

with $q_0, q_1, q_2, q_3 \in \mathbb{R}$.

The summation of quaternions is defined by the addition of 4-tuples $Q + P = (q_0 + p_0, q_i + p_i)$. However, as Eq. (2.48) shows the multiplication is not commutative, contrary to the field \mathbb{C} . For two elements $P, Q \in \mathbb{H}$ the multiplication, the *Hamilton* product, is defined by

$$\begin{aligned} PQ &= P \odot Q = (p_0, \vec{p}) \odot (q_0, \vec{q}) \\ &= (p_0 + ip_1 + jp_2 + kp_3)(q_0 + iq_1 + jq_2 + kq_3) \\ &= (p_0q_0 - p_1q_1 - p_2q_2 - p_3q_3) + i(p_0q_1 + p_1q_0 + p_2q_3 - p_3q_2) \\ &\quad + j(p_0q_2 - p_1q_3 + p_2q_0 + p_3q_1) + k(p_0q_3 + p_1q_2 - p_2q_1 + p_3q_0) \\ &= (p_0q_0 - \vec{p} \cdot \vec{q}, q_0\vec{p} + p_0\vec{q} + (\vec{p} \times \vec{q})) \end{aligned} \quad (2.50)$$

denoting for the readers convenience the quaternion multiplication with the symbol " \odot ".

2.5.1 Norm and conjugation

Since $q_0 = \Re[Q]$ in Eq. (2.49) is a real number it is denoted *scalar part* or *real part* of quaternions. The *pure imaginary part* $iq_1 + jq_2 + kq_3 = \Im[Q]$ is also denoted *vector part*. For each quaternion Q there is a conjugated quaternion $\bar{Q} \equiv Q^* = (q_0, -q_i)$. If $Q = \bar{Q}$ then the quaternion Q is a real or *scalar* quaternion and if $Q = -\bar{Q}$, it is a pure imaginary quaternion.

Furthermore there exists a scalar product: For two quaternions $P, Q \in \mathbb{H}$, we define

$$\langle P, Q \rangle = P \cdot Q = \Re[\bar{P}Q] = \Re[\bar{Q}P] \quad (2.51)$$

and the norm is written

$$\|Q\| = \sqrt{\langle Q, Q \rangle} = \sqrt{Q \cdot \bar{Q}} = \sqrt{\bar{Q} \cdot Q} \geq 0. \quad (2.52)$$

This is always a non-negative real number $\|Q\| \in \mathbb{R}_0^+$ and hence it is possible to define a metric on \mathbb{H} . With a distance function $d : \mathbb{H} \mapsto \mathbb{R}_0^+$ of two quaternions $P, Q \in \mathbb{H}$

$$d(P, Q) = \|P - Q\|. \quad (2.53)$$

With the above tools we are introducing *unit* quaternions with the norm $\|Q\| = Q\bar{Q} = 1$. Every product of two normalised quaternions is also a normalised quaternion. Consequently, the inverse element of an arbitrary quaternion is calculated to

$$Q^{-1} = \frac{\bar{Q}}{\|Q\|^2}. \quad (2.54)$$

For a unit quaternions Q follows $Q^{-1} = \bar{Q}$. Unit quaternions form a non-commutative group. Geometrically, unit quaternions define a sphere \mathcal{S}^3 in \mathbb{R}^4 . As shown later unit quaternions are a *Lie*-group.

2.5.2 Rotations

By help of unit quaternions there is an elegant method to describe rotations in \mathbb{R}^3 . Regarding a vector $\vec{v} \in \mathcal{V} \subseteq \mathbb{R}^3$ as the vector part of a pure quaternion⁹ $(0, \vec{v}) \in \mathbb{H}_p$, there exists a function R_Q with $Q \in \mathbb{H}$, which describes a rotation around an axis $q_i = \Im[Q]$ with an angle of $q_0 = \Re[Q]$ in \mathbb{R}^3 :

$$R_Q : \begin{cases} \mathbb{H} \mapsto \mathbb{H}_p \\ R_Q(\vec{v}) = Q \vec{v} Q^{-1} \equiv Q \odot (0, \vec{v}) \odot Q^{-1} \end{cases} \quad (2.55)$$

Compositions of rotations corresponds to multiplication of quaternions. Consider two quaternions $P, Q \in \mathbb{H}$ acting on an arbitrary vector $\vec{v} \in \mathbb{H}_p$, then

$$\begin{aligned} R_{PQ}(\vec{v}) &= R_P(R_Q(\vec{v})) = R_P(Q \vec{v} Q^{-1}) \\ &= PQ \vec{v} Q^{-1} P^{-1} = PQ \vec{v} (PQ)^{-1} = R_{PQ}(\vec{v}). \end{aligned} \quad (2.56)$$

The inverse of a rotation R_Q^{-1} corresponds to a rotation $R_{Q^{-1}}$ in opposite direction, expressed by a quaternion $Q^{-1} = \bar{Q} = Q^*$. Therefore it is

$$R_Q^{-1} = R_{Q^{-1}} \quad (2.57)$$

and subsequently, there is an homomorphism between the group \mathcal{S}^3 of quaternions and the Lie-group $\mathbf{SO}(3)$ of rotations. The mapping R

$$R : \begin{cases} \mathcal{S}^3 & \mapsto \mathbf{SO}(3) \\ Q & \mapsto R_Q \end{cases}$$

is a twofold covering of $\mathbf{SO}(3)$, because any element $R_Q \in \mathbf{SO}(3)$ consists of two preimages $\pm Q \in \mathcal{S}^3$.

⁹The vector \vec{v} is also considered as an element of the group \mathbb{H}_p , which is a subgroup of \mathbb{H}

$$\mathbb{H}_p = \left\{ Q \in \mathbb{H} \mid \Re[Q] = 0 \right\}.$$

For better understanding, the explicit representation of a rotational matrix $D_{ij}(\omega) \in \mathbf{SO}(3)$ will be shown. Repeating *Rodrigues' rotation formula*, a vector $\vec{v} \in \mathcal{V} \subseteq \mathbb{R}^3$ transforms to \vec{v}' by rotating around an axis $\vec{\omega}$ and an angle $\omega = \|\vec{\omega}\|$

$$\vec{v}' = \vec{v} + (1 - \cos \omega) \vec{\omega} \times (\vec{\omega} \times \vec{v}) + \sin \omega (\vec{\omega} \times \vec{v}). \quad (2.58)$$

This relation can be expressed in matrix notation

$$v'_i = \sum_{j=1}^3 D_{ij}(\omega) v_j \quad (2.59)$$

with

$$D_{ij}(\omega) = \delta_{ij} \cos \omega + \omega_i \omega_j (1 - \cos \omega) - \sin \omega \sum_{k=1}^3 \varepsilon_{ij}^k \omega_k, \quad (2.60)$$

$\omega_i = \frac{\vec{\omega}}{\|\vec{\omega}\|} \vec{e}_i$ and unit vectors \vec{e}_i .

The same rotation can be formulated in quaternionic notation with the vector $\vec{v} \in \mathcal{V} \subseteq \mathbb{R}^3$ represented by the pure quaternion $V_{\mathbb{H}} = (0, \vec{v})$ and the rotation by the unit quaternion $Q \in \mathbb{H}$

$$QV_{\mathbb{H}} = (q_0, \vec{q})(0, \vec{v}) = (q_0 \cdot 0 - \vec{q}\vec{v}, q_0\vec{v} + 0 \cdot \vec{q} + \vec{q} \times \vec{v}) \quad (2.61)$$

$$V'_{\mathbb{H}} = QV_{\mathbb{H}}Q^{-1} = \left(0, \underbrace{\vec{v} + 2q_0(\vec{q} \times \vec{v}) + 2\vec{q} \times (\vec{q} \times \vec{v})}_{\vec{v}'}\right). \quad (2.62)$$

The corresponding rotation matrix reads

$$D_{ij}(\omega) = \begin{pmatrix} 1 - 2q_2^2 - 2q_3^2 & -2q_0q_3 + 2q_1q_2 & 2q_0q_2 + 2q_1q_3 \\ 2q_0q_3 + 2q_1q_2 & 1 - 2q_1^2 - 2q_3^2 & -2q_0q_1 + 2q_2q_3 \\ -2q_0q_2 + 2q_1q_3 & 2q_0q_1 + 2q_2q_3 & 1 - 2q_1^2 - 2q_2^2 \end{pmatrix}. \quad (2.63)$$

The matrices $D_{ij}(\omega)$ in equations (2.60) and (2.63) are equal, if we consider the quaternion $Q = \exp[i\vec{n}\frac{\omega}{2}]$ with $\|\vec{n}\| = \vec{n}\vec{n}^* = 1$ and $\vec{n} = \frac{\vec{\omega}}{\|\vec{\omega}\|}$. Using the generalised *Euler formula*, we obtain

$$\begin{aligned} V'_{\mathbb{H}} &= (0, \vec{v}') = QV_{\mathbb{H}}Q^{-1} = e^{\frac{i}{2}\vec{n}\omega} \odot V_{\mathbb{H}} \odot e^{-\frac{i}{2}\vec{n}\omega} \\ &= \left(\cos \frac{\omega}{2} + i\vec{n} \sin \frac{\omega}{2}\right) \odot (0, \vec{v}) \odot \left(\cos \frac{\omega}{2} - i\vec{n} \sin \frac{\omega}{2}\right). \end{aligned} \quad (2.64)$$

Expanding Eq. (2.64)

$$\vec{v}' = \vec{v} \cos^2 \frac{\omega}{2} + (\vec{n} \odot \vec{v} - \vec{v} \odot \vec{n}) \sin \frac{\omega}{2} \cos \frac{\omega}{2} - \vec{n} \odot \vec{v} \odot \vec{n} \sin^2 \frac{\omega}{2} \quad (2.65)$$

where $\vec{n} \odot \vec{v}$ means quaternion multiplication¹⁰. Thus, we calculate

$$\begin{aligned}\vec{n} \odot \vec{v} - \vec{v} \odot \vec{n} &= \left(-\vec{n} \cdot \vec{v}, \vec{n} \times \vec{v} \right) - \left(-\vec{v} \cdot \vec{n}, \vec{v} \times \vec{n} \right) \\ &= \left(0, 2(\vec{n} \times \vec{v}) \right) = 2(\vec{n} \times \vec{v})\end{aligned}\quad (2.67)$$

and

$$\begin{aligned}\vec{n} \odot \vec{v} \odot \vec{n} &= \left(0, \vec{n} \right) \odot \left(-\vec{v} \cdot \vec{n}, \vec{v} \times \vec{n} \right) \\ &= \left(-\vec{n} \cdot (\vec{v} \times \vec{n}), -(\vec{v} \cdot \vec{n})\vec{n} + \vec{n} \times (\vec{v} \times \vec{n}) \right).\end{aligned}\quad (2.68)$$

Using $\vec{n} \cdot (\vec{v} \times \vec{n}) = 0$ and $\vec{n} \times (\vec{v} \times \vec{n}) = \varepsilon_{ijk}n_j\varepsilon_{klm}v_l n_m = v_i(n_j n_j) - n_i(v_j n_j)$, that is, applied on Eq. (2.68)

$$\begin{aligned}\vec{n} \odot \vec{v} \odot \vec{n} &= \left(0, -(v_j n_j)n_i + v_i \underbrace{(n_j n_j)}_1 - n_i(v_j n_j) \right) \\ &= \left(0, v_i - 2n_i(v_j n_j) \right) = \left(0, \vec{v} - 2\vec{n}(\vec{v} \cdot \vec{n}) \right)\end{aligned}\quad (2.69)$$

Now, inserting Eq. (2.67) and (2.69) in Eq. (2.65), we obtain

$$\begin{aligned}\vec{v}' &= \vec{v} \cos^2 \frac{\omega}{2} + 2(\vec{n} \times \vec{v}) \sin \frac{\omega}{2} \cos \frac{\omega}{2} - (\vec{v} - 2\vec{n}(\vec{v} \cdot \vec{n})) \sin^2 \frac{\omega}{2} \\ &= \vec{v} \underbrace{\left(\cos^2 \frac{\omega}{2} - \sin^2 \frac{\omega}{2} \right)}_{\cos \omega} + (\vec{n} \times \vec{v}) \underbrace{\left(2 \sin \frac{\omega}{2} \cos \frac{\omega}{2} \right)}_{\sin \omega} + \vec{n}(\vec{v} \cdot \vec{n}) \underbrace{\left(2 \sin^2 \frac{\omega}{2} \right)}_{1 - \cos \omega} \\ &= \vec{v} \cos \omega + \vec{n}(\vec{v} \cdot \vec{n})(1 - \cos \omega) + (\vec{n} \times \vec{v}) \sin \omega\end{aligned}\quad (2.70)$$

As mentioned above, this result is equal to *Rodrigues' rotation formula* Eq. (2.58) and the rotation matrix (2.60) written in index notation.

There is also an isomorphism between the Lie-group or *spin-group* $\mathbf{SU}(2)$ and the group of unit quaternions, covering a unit sphere \mathcal{S}^3 . If we consider the Pauli matrices σ_i and map them to a basis representation of \mathcal{S}^3 with $\{\mathbb{1}_{\mathbb{H}}, i_{\mathbb{H}}, j_{\mathbb{H}}, k_{\mathbb{H}}\}$, we introduce

$$\mathbb{1}_{\mathbb{H}} = \mathbb{1}_2, \quad i_{\mathbb{H}} = -i\sigma_1, \quad j_{\mathbb{H}} = -i\sigma_2, \quad k_{\mathbb{H}} = -i\sigma_3 \quad (2.71)$$

and are able to write quaternions $Q \in \mathbb{H}$ as

$$Q = \left(q_0, \vec{q} \right) = q_0 \mathbb{1}_2 - i\sigma_K q_K \quad (2.72)$$

$$= \begin{pmatrix} q_0 - iq_3 & -q_2 - iq_1 \\ q_2 - iq_1 & q_0 + iq_3 \end{pmatrix} = \begin{pmatrix} w & -\bar{z} \\ z & \bar{w} \end{pmatrix} = U \quad (2.73)$$

¹⁰Again using Eq. (2.50), a pure quaternion multiplication connotes

$$\begin{aligned}\vec{n} \odot \vec{v} &= (0, n_i) \odot (0, v_i) = (-n_i v_i, \varepsilon_{klm} n_l v_m) \\ &= \vec{n} \times \vec{v} - \vec{n} \cdot \vec{v}\end{aligned}\quad (2.66)$$

where the second line is written in a sloppy notation.

with the imaginary unit $i^2 = -1$. The elements $q_0, q_i \in \mathbb{R}$ are real, subsequently $w, z \in \mathbb{C}$ are considered complex. The determinant of these 2×2 -matrices U is $+1$.

$$\det[U] = \|w\|^2 + \|z\|^2 = q_0^2 + q_1^2 + q_2^2 + q_3^2 = 1 \quad (2.74)$$

That means, the matrices U belong to the Lie-group $\mathbf{SU}(2)$ and are generators of spin rotations. For informational purposes, these elements of $\mathbf{SU}(2)$ are representable by a set of *Euler angles* $\{\phi, \theta, \psi\}$

$$\begin{aligned} U(\phi, \theta, \psi) &= U_{z'}(\phi)U_y(\theta)U_z(\psi) = e^{i\sigma_3\frac{\phi}{2}}e^{i\sigma_2\frac{\theta}{2}}e^{i\sigma_3\frac{\psi}{2}} \\ &= \begin{pmatrix} \cos\frac{\theta}{2}e^{i\frac{\psi+\phi}{2}} & \sin\frac{\theta}{2}e^{-i\frac{\psi-\phi}{2}} \\ -\sin\frac{\theta}{2}e^{i\frac{\psi-\phi}{2}} & \cos\frac{\theta}{2}e^{-i\frac{\psi+\phi}{2}} \end{pmatrix} \end{aligned} \quad (2.75)$$

with $0 \leq \theta \leq \pi, 0 \leq \phi \leq 2\pi$ and $0 \leq \psi \leq 4\pi$ ([13] page 25).

2.5.3 Derivative

With the help of the four unit vectors (2.71), (2.72) and $Q(s) \in \mathbf{SU}(2)$ it is possible to define a tangent space at every point of the unit sphere $\mathcal{S}^3 \subset \mathbb{R}^4$. The vectors

$$\mathbb{1}_2 Q(s) = Q(s), \quad \sigma_K Q(s) = \sigma_K^Q \quad (2.76)$$

with $K = 1, 2, 3$ span a orthonormal basis, where $Q(s)$ describe a point of the unit sphere \mathcal{S}^3 and σ_K^Q is the inherent tangent space \mathcal{TS}^3 at this point. Building the scalar product between these vectors, we see

$$Q(s) \cdot \sigma_K Q(s) = \frac{1}{2} \text{Tr} \left[\underbrace{Q(s)Q^\dagger(s)}_1 \underbrace{\sigma_K^\dagger}_{\sigma_K} \right] = \frac{1}{2} \text{Tr} [\sigma_K] = 0 \quad (2.77)$$

$$\sigma_K Q(s) \cdot \sigma_L Q(s) = \frac{1}{2} \text{Tr} \left[\sigma_K Q(s)Q^\dagger(s)\sigma_L^\dagger \right] = \frac{1}{2} \text{Tr} \left[\underbrace{\sigma_K \sigma_L}_{\delta_{KL}} \right] = \delta_{KL} \quad (2.78)$$

the orthogonality.

Regarding a path $x^\mu(s)$ in four-dimensional Minkovski space, parameterised by s , a quaternion field $Q(s)$ defines a corresponding path on a sphere $\mathcal{S}^3 \subset \mathbb{R}^4$ along s . The derivative of $Q(s)$ is

$$\partial_s Q(s) = \lim_{\Delta s \rightarrow 0} \frac{Q(s + \Delta s) - Q(s)}{\Delta s} \quad (2.79)$$

a vector in tangent space \mathcal{TS}^3 at $Q(s)$. Therefore, it is possible to write $\partial_s Q(s)$ as a linear combination of unit vectors $\sigma_K^Q = \sigma_K Q$ with the coefficients Γ_{sK}

$$\partial_s Q(s) = -i \sum_{K=1}^3 \Gamma_{sK} \sigma_K^Q \equiv -i \Gamma_{sK} \sigma_K Q. \quad (2.80)$$

Again using the representation (2.72) of quaternions, the coefficients¹¹ Γ_{sK} are written explicitly

$$\begin{aligned}\partial_s Q(s)Q^\dagger(s) &= -i\sigma_K \underbrace{\left(q_0\partial_s q_K - q_K\partial_s q_0 + \varepsilon_{KLM}q_Lq_M \right)}_{\Gamma_{sK}} \\ \Gamma_{sK} &= q_0\partial_s q_K - q_K\partial_s q_0 + \varepsilon_{KLM}q_Lq_M\end{aligned}$$

and according to (2.80) in general form

$$\Gamma_{sK} = \frac{i}{2} \text{Tr} \left[\partial_s Q Q^\dagger \sigma_K \right]. \quad (2.81)$$

The modification of local unit vectors σ_K^Q of the tangent space along a parametric path s will be obtained as well by a directional derivative using expression (2.80)

$$\begin{aligned}\partial_s \sigma_K^Q &= \sigma_K \partial_s Q(s) = -i\sigma_K \Gamma_{sL} \sigma_L Q(s) \\ &= \varepsilon_{KLM} \Gamma_{sL} \sigma_M^Q - i\delta_{KL} \Gamma_{sL} Q.\end{aligned} \quad (2.82)$$

The directional derivative of the local unit vectors exhibits components in tangent direction as well as in normal direction. If we use the generators of $\mathbf{SU}(2)$ in the *fundamental* representation, see Eq. (2.47)

$$T_K = -i\varepsilon_K \equiv -i(\varepsilon_K)_{LM} = -i\varepsilon_{KLM} \quad (2.83)$$

Eq. (2.82) becomes

$$\begin{aligned}\partial_s \sigma_K^Q &= \underbrace{(\varepsilon_K)_{LM}}_{-(\varepsilon_L)_{KM}} \Gamma_{sL} \sigma_M^Q - i\Gamma_{sK} Q = -i((T_L)_{KM} \Gamma_{sL}) \sigma_M^Q - i\Gamma_{sK} Q \\ &= -i\Gamma_{sKM} \sigma_M^Q - i\Gamma_{sK} Q\end{aligned} \quad (2.84)$$

with $\Gamma_{sKM} = -i(\varepsilon_L \Gamma_{sL})_{KM} = -i\varepsilon_{LKM} \Gamma_{sL} \equiv T_L \Gamma_{sL}$, denoted *affine connection coefficient*.¹²

¹¹Using the Hamilton product in

$$\begin{aligned}\partial_s Q(s)Q^\dagger(s) &= (\partial_s(q_0, q_K)) \odot (q_0, -q_L) = \left(\partial_s q_0 - i\sigma_K \partial_s q_K \right) \left(q_0 + i\sigma_L q_L \right) \\ &= q_0 \partial_s q_0 - i\sigma_K \partial_s q_K q_0 + i\sigma_L q_L \partial_s q_0 + \sigma_K \sigma_L \partial_s q_K q_L\end{aligned}$$

and with the identity $\sigma_K \sigma_L = \delta_{KL} + i\varepsilon_{KLM} \sigma_M$ we get

$$\partial_s Q(s)Q^\dagger(s) = \underbrace{q_0 \partial_s q_0 + \delta_{KL} q_L \partial_s q_K}_0 - i\sigma_K (q_0 \partial_s q_K - q_K \partial_s q_0 + \varepsilon_{KLM} q_L \partial_s q_M).$$

¹²The affine connection coefficients correspond to Christoffel symbols in general relativity which can be derived from the metric tensor g_{ij} by

$$\Gamma_{ijk} = \frac{1}{2} (\partial_j g_{ik} + \partial_k g_{ij} - \partial_i g_{jk})$$

The derivative of a vector field $v(s) = \sigma_K^{Q(s)} v_K(s)$

$$\begin{aligned}
\partial_s v(s) &= \sigma_K^Q \partial_s v_K(s) + \partial_s \sigma_K^Q v_K(s) \\
&= \sigma_K^Q \partial_s v_K(s) - \underbrace{i \Gamma_{sKM} \sigma_M^Q v_K(s)}_{-\sigma_K^Q \Gamma_{sKM} v_M(s)} - i \Gamma_{sK} Q(s) v_K(s) \\
&= \sigma_K^Q \left[\underbrace{\delta_{KM} \partial_s + i \Gamma_{sKM}}_{(D_s)_{KM}} \right] v_M(s) - i \Gamma_{sK} v_K(s) Q(s) \quad (2.85)
\end{aligned}$$

shows how we have to define the *covariant derivative* $(D_s)_{KM} = \partial_s \delta_{KM} + i \Gamma_{sKM}$. If the covariant derivative of a vector field vanishes $(D_s)_{KM} v_M(s) = 0$, the vector field is called *parallel* or *parallel transported* along the path parametrised by s . In this case the modification of the vector field v_K between s and $s + ds$

$$\begin{aligned}
v_K(s + ds) &= v_K(s) + ds \partial_s v_K(s) \\
&= (\delta_{KM} - i \Gamma_{sKM} ds) v_M(s) = e^{-i \Gamma_{sKM} ds} v_M(s) \quad (2.86)
\end{aligned}$$

is given by

$$\partial_s v_K(s) ds = -i \Gamma_{sKM} v_M(s) ds \quad (2.87)$$

Geometrically the affine connection Γ_{sKM} can be interpreted as the velocity of the rotating local Dreibein as well as the velocity of the variation of the point $Q(s)$ on the manifold — in this case on the sphere \mathcal{S}^3 .

2.5.4 Curvature

In differential geometry curvature tensors describe the curvature of Riemannian manifolds. We can define the curvature tensors R by using the affine connections and covariant derivatives. We derive the Riemannian Tensor at $Q \in \mathbf{SU}(2)$ from

$$\partial_s \partial_t \sigma_K^Q - \partial_t \partial_s \sigma_K^Q \quad (2.88)$$

Using (2.80) we derive (2.84) again and get

$$\partial_t \partial_s \sigma_K^Q = -i \partial_t (\Gamma_{sKL} \sigma_L^Q + \Gamma_{sK} Q) \quad (2.89)$$

$$= -i (\partial_t \Gamma_{sKM} - i \Gamma_{sKL} \Gamma_{tLM} - i \Gamma_{sK} \Gamma_{tM}) \sigma_M^Q - i (\partial_t \Gamma_{sK} - i \Gamma_{sKL} \Gamma_{tL}) Q$$

$$\partial_s \partial_t \sigma_K^Q = -i \partial_s (\Gamma_{tKL} \sigma_L^Q + \Gamma_{tK} Q) \quad (2.90)$$

$$= -i (\partial_s \Gamma_{tKM} - i \Gamma_{tKL} \Gamma_{sLM} - i \Gamma_{tK} \Gamma_{sM}) \sigma_M^Q - i (\partial_s \Gamma_{tK} - i \Gamma_{tKL} \Gamma_{sL}) Q$$

The difference $\partial_s \partial_t \sigma_K^Q - \partial_t \partial_s \sigma_K^Q$ has radial components in direction Q and components in the tangent space at Q defining the curvature tensor

$$R_{KM}(s, t) = -i (\partial_s \Gamma_{tKM} - \partial_t \Gamma_{sKM} + \Gamma_{tKL} \Gamma_{sLM} - \Gamma_{sKL} \Gamma_{tLM}). \quad (2.91)$$

Inserting the generators T_K from Eq. (2.47) and (2.83)

$$\begin{aligned}
\Gamma_{tKL}\Gamma_{sLM} - \Gamma_{sKL}\Gamma_{tLM} &= T_{PKL}\Gamma_{tP}T_{RLM}\Gamma_{sR} - T_{RKL}\Gamma_{sR}T_{PLM}\Gamma_{tP} \\
&= [T_{PKL}T_{RLM} - T_{RKL}T_{PLM}]\Gamma_{sR}\Gamma_{tP} \\
&= [(T_P T_R)_{KM} - (T_R T_P)_{KM}]\Gamma_{sR}\Gamma_{tP} \\
&= [T_P, T_R]_{KM}\Gamma_{sR}\Gamma_{tP}
\end{aligned} \tag{2.92}$$

and the commutator (2.46) of the Lie-algebra $\mathfrak{su}(2)$ results in

$$\Gamma_{tKL}\Gamma_{sLM} - \Gamma_{sKL}\Gamma_{tLM} = i\varepsilon_{PRN}T_{NKM}\Gamma_{sR}\Gamma_{tP}. \tag{2.93}$$

Inserting Eq. (2.93) in (2.91) the curvature tensor is

$$\begin{aligned}
R_{stKM} &= -i(\partial_s\Gamma_{tP}T_{PKM} - \partial_t\Gamma_{sP}T_{PKM} + iT_{NKM}\varepsilon_{PRN}\Gamma_{sR}\Gamma_{tP}) \\
&= T_{NKM}(\partial_s\Gamma_{tN} - \partial_t\Gamma_{sN} - \varepsilon_{RPN}\Gamma_{sR}\Gamma_{tP}).
\end{aligned} \tag{2.94}$$

Here we can see an important difference to *general relativity*, where the Riemannian curvature tensor has four space-time indices. In contrast, the indices K and M in R_{stKM} refer to the internal space \mathcal{S}^3 and only the indices s and t are space-time indices.

For the contribution in Q -direction in Eq. (2.89) we use *Schwarz' theorem*

$$\begin{aligned}
\partial_s\Gamma_{tK} - \partial_t\Gamma_{sK} &= i(\Gamma_{tKL}\Gamma_{sL} - \Gamma_{sKL}\Gamma_{tL}) \\
&= i(T_{MKL}\Gamma_{tM}\Gamma_{sL} - T_{MKL}\Gamma_{sM}\Gamma_{tL}) \\
&= 2iT_{KLM}\Gamma_{sL}\Gamma_{tM}
\end{aligned} \tag{2.95}$$

and with $T_{KLM} = -i\varepsilon_{KLM}$ we derive the *Maurer-Cartan equation*

$$\partial_s\Gamma_{tK} - \partial_t\Gamma_{sK} = 2\varepsilon_{KLM}\Gamma_{sL}\Gamma_{tM}. \tag{2.96}$$

The *Maurer-Cartan equation* is an extra constraint for the affine connection field Γ_{sK} and guarantees the uniqueness of quaternion fields in space-time.

Combining (2.96) with (2.94) the curvature tensor reads

$$R_{stKM} = T_{NKM} \underbrace{\frac{1}{2}(\partial_s\Gamma_{tN} - \partial_t\Gamma_{sN})}_{R_{stN}} \tag{2.97}$$

or shorter

$$R_{stKM} = T_{NKM} \underbrace{\varepsilon_{NPR}\Gamma_{sP}\Gamma_{tR}}_{R_{stN}} = T_{NKM}R_{stN} \tag{2.98}$$

with R_{stN} as components of a vector \vec{R}_{st} .

Chapter 3

Model of topological fermions

The transition from differential geometry to physical quantities can be done by identifying the curvature tensor R_{stKM} with the electrical field tensor $F_{\mu\nu}$ and the affine connection Γ_{sK} with the dual gauge field A_μ . We derive the affine connection from the soliton-field $Q(x)$. Referring to the international unit system (SI), we define the dual gauge field $C_{\mu K}$

$$C_{\mu K} = -\frac{e_0}{4\pi\epsilon_0 c}\Gamma_{\mu K} = -\frac{\alpha_f \hbar}{e_0}\Gamma_{\mu K} \quad (3.1)$$

with the *fine-structure constant*¹ $\alpha_f = \frac{1}{4\pi\epsilon_0} \frac{e_0^2}{\hbar c}$ as well as the *dual (electromagnetic) field strength tensor* $*F_{\mu\nu}$

$$*F_{\mu\nu KM} = T_{PKM} \frac{1}{2} (\partial_\mu C_{\nu P} - \partial_\nu C_{\mu P}) = -\frac{e_0}{4\pi\epsilon_0 c} R_{\mu\nu KM}. \quad (3.2)$$

Formally, the dual field strength tensor has the same form as in electrodynamics or more precise as in QCD because of the additional internal indices K and M

$$*F_{\mu\nu KM} = T_{KMP} \frac{1}{c} \begin{pmatrix} 0 & cB_{1P} & cB_{2P} & cB_{3P} \\ -cB_{1P} & 0 & E_{3P} & -E_{2P} \\ -cB_{2P} & -E_{3P} & 0 & E_{1P} \\ -cB_{3P} & E_{2P} & -E_{1P} & 0 \end{pmatrix}. \quad (3.3)$$

According to equations (3.1) and (3.2) the electromagnetic flux through a infinitesimal parallelogram $*F_{\mu\nu} dx^\mu dx^\nu$ is proportional to the area of an infinitesimal parallelogram in the internal space, or inspired by QCD often denoted as *color space*

$$(*F_{\mu\nu})_{KM} dx^\mu dx^\nu \sim R_{\mu\nu KM} dx^\mu dx^\nu = T_{NKM} \epsilon_{NPR} \Gamma_{\mu P} \Gamma_{\nu R} dx^\mu dx^\nu. \quad (3.4)$$

¹Based on [21], the currently accepted value of fine-structure constant α_f is

$$\alpha_f = 7.2973525664(17) \times 10^{-3} \approx \frac{1}{137.036}.$$

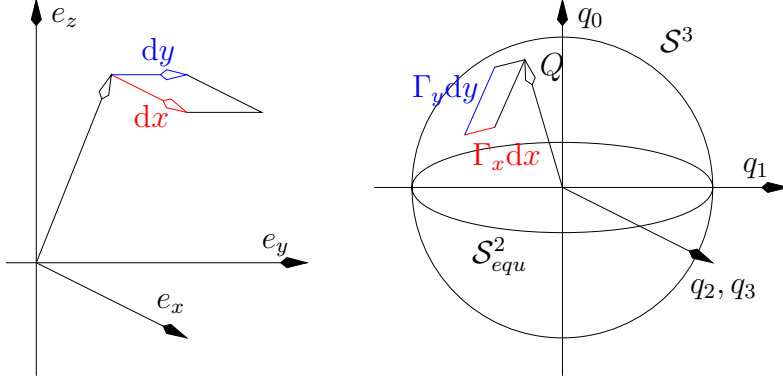


Figure 3.1: Shape of an infinitesimal parallelogram in the tangent space of the \mathcal{S}^3 -sphere at $Q(x^\mu)$, spanned by two affine connection vectors $\varepsilon_{KPR}\Gamma_{\mu P}\Gamma_{\nu R}$.

3.1 Hedgehog approach

Based on this geometrical analogy (3.4), particles like electrically charged monopoles (electrons, positrons) can be represented by solitonic excitations of non-Abelian fields. We will use a hedgehog-ansatz for the elements of an $\mathbf{SU}(2)$ -field $Q(x)$

$$Q(r) = \underbrace{\cos \alpha(r)}_{q_0} - i\sigma_K \underbrace{n_K \sin \alpha(r)}_{q_K} \quad \text{and} \quad \alpha(r) \in \left[0, \frac{\pi}{2}\right], \quad (3.5)$$

with $n_K = \frac{r_K}{r}$ and $\|n_K\| = 1$. The profile function $\alpha = \alpha(r)$ has to vanish at the origin $\alpha(0) = 0$, eliminating the singularity at $r = 0$ and is running monotonically to $\pi/2$ at infinity,

$$\alpha(0) = 0, \quad \lim_{r \rightarrow \infty} \alpha(r) = \frac{\pi}{2}. \quad (3.6)$$

That means, the soliton field $Q(x)$ is taking values on the unit sphere \mathcal{S}^3 . In the *electrodynamic limit*, that means far away from the soliton centre ($r \gg 0$), the soliton field component q_0 of Eq. (3.1) approaches zero, $q_0 \mapsto 0$ and the components q_K to the unit vector n_K , $q_K \mapsto n_K$. At infinity, the soliton field $Q(x)$ is restricted to the equator of the unit sphere \mathcal{S}^3 , a two dimensional submanifold $\mathcal{S}_{\text{equ}}^2 \in \mathcal{S}^3$.

In the electrodynamic limit, we get the mapping \mathcal{S}_∞^2 to $\mathcal{S}_{\text{equ}}^2$. Such mappings are divided into homotopy classes, characterised by a non-negative integer $Z = \pi_2(\mathcal{S}^2)$. The integer Z describes the number of coverings of $\mathcal{S}_{\text{equ}}^2$ by \mathcal{S}_∞^2 [14] and is a topology invariant. We call it *number of windings* w_s

$$w_s = \frac{1}{4\pi} \oint_{\mathcal{S}^2} n_K [\varepsilon_{KLM} \partial_\theta n_L \partial_\varphi n_M] d\theta d\varphi. \quad (3.7)$$

There is another quantum number, denoted *topological charge* \mathcal{Q} . It counts the number of coverings of the internal- or *colour* space \mathcal{S}^3 . It is defined by

$$\mathcal{Q} = \frac{1}{V(\mathcal{S}^3)} \int_{\mathbb{R}^3} d^3r \varepsilon_{KLM} \Gamma_{1K} \Gamma_{2L} \Gamma_{3M} \quad (3.8)$$

with

$$V(\mathcal{S}^3) = \int_{\mathcal{S}^3} dQ. \quad (3.9)$$

As mentioned in 2.5.3, the three vectors $\Gamma_{iK} dx^i$ define an infinitesimal parallelepiped on \mathcal{S}^3 with the volume given by the scalar triple product

$$\varepsilon_{KLM} \Gamma_{1K} \Gamma_{2L} \Gamma_{3M} \Big|_p dx^1 dx^2 dx^3$$

These quantum numbers, w_s and \mathcal{Q} , can be assigned to electrical charge q_{el} and spin quantum number s , respectively.

$$q_{el} = -e_0 w_s \quad (3.10)$$

$$s = |\mathcal{Q}| \quad (3.11)$$

3.1.1 Affine connection

For now, we explicitly want to calculate the affine connections Γ_{sK} for the hedgehog approach. According to the ansatz (3.5) and using the derivative (2.81), one obtains

$$\partial_s Q Q^\dagger = -i \sigma_K \left[\underbrace{n_K \partial_s \alpha + \sin \alpha \cos \alpha \partial_s n_K + \varepsilon_{KLM} n_L \partial_s n_M}_{\Gamma_{sK}} \right]. \quad (3.12)$$

In spherical coordinates Eq. (3.12) reads

$$\begin{aligned} \Gamma_{rK} &= n_K \partial_r \alpha(r) = e_{rK} \partial_r \alpha(r), \\ \Gamma_{\vartheta K} &= \sin \alpha [\cos \alpha e_{\vartheta K} + \sin \alpha e_{\varphi K}] = \sin \alpha e_{\zeta K}, \\ \Gamma_{\varphi K} &= \sin \alpha \sin \vartheta [\cos \alpha e_{\varphi K} - \sin \alpha e_{\vartheta K}] = \sin \alpha \sin \vartheta e_{\eta K}, \end{aligned} \quad (3.13)$$

with the unit vectors in colour space $e_{rK}, e_{\vartheta K}, e_{\varphi K}$ as well as the shortcuts $e_{\zeta K} = \cos \alpha e_{\vartheta K} + \sin \alpha e_{\varphi K}$ and $e_{\eta K} = \cos \alpha e_{\varphi K} - \sin \alpha e_{\vartheta K}$. Inserting the connections (3.13) in Eqs. (3.1), (3.3), the electric field E_i is in spherical components given by

$$\begin{aligned} E_{rK} &= -\frac{\alpha_f \hbar}{e_0} \frac{\varepsilon_{KLM} \Gamma_{\vartheta L} \Gamma_{\varphi M}}{l_\vartheta l_\varphi} = -\frac{\alpha_f \hbar \sin^2 \alpha}{e_0 r^2} e_{rK}, \\ E_{\vartheta K} &= -\frac{\alpha_f \hbar}{e_0} \frac{\varepsilon_{KLM} \Gamma_{\varphi L} \Gamma_{rM}}{l_\varphi l_r} = -\frac{\alpha_f \hbar \partial_r \alpha(r) \sin \alpha}{e_0 r} e_{\zeta K}, \\ E_{\varphi K} &= -\frac{\alpha_f \hbar}{e_0} \frac{\varepsilon_{KLM} \Gamma_{rL} \Gamma_{\vartheta M}}{l_r l_\vartheta} = -\frac{\alpha_f \hbar \partial_r \alpha(r) \sin \alpha}{e_0 r} e_{\eta K}, \end{aligned} \quad (3.14)$$

where we used the length scales $(l_r, l_\vartheta, l_\varphi) = (1, r, r \sin \vartheta)$ in spherical coordinates.

Due to the properties (3.6) of the profile function the components E_{iK} of Eq. (3.14) vanish at infinity. It is interesting to see that the only surviving component

$$E_{rK} \rightarrow -\frac{\alpha_f \hbar}{\epsilon_0} \frac{1}{r^2} e_{rK}, \quad E_{\theta K} \rightarrow 0, \quad E_{\phi K} \rightarrow 0 \quad (3.15)$$

approaches at infinity the well known r^{-2} -behaviour of *Coulomb* field of electric charges.

The total electric field energy H_e is calculated by integration of the energy density over the whole volume, that is with Eq. (3.14)

$$\begin{aligned} H_e &= \int_V d^3r \mathcal{H}_e = \frac{\epsilon_0}{2} \int_V d^3r E_{iK} E_K^i \\ &= \alpha_f \hbar c \int_0^\infty dr \left[\frac{\sin^4 \alpha}{2r^2} + (\partial_r \cos \alpha)^2 \right]. \end{aligned} \quad (3.16)$$

3.2 Lagrangian density

In analogy to the electrodynamic field theory, we define a Lagrangian density in the *model of topological fermions* (MTF). To describe experimental properties, the solitons have to be steady and stable, being able to be interpreted as charged particles (ie.: electrons) within a Coulomb-field. Since solitons and their field are described by the same degrees of freedom, there is no need for explicit source terms which are necessary in Maxwell's electrodynamics. The Lagrangian density \mathcal{L} will consist of two competing parts, on one hand a term \mathcal{L}_{kin} , well-known in field theories, quadratic in the field strength without electromagnetic sources and on the other hand a potential term \mathcal{L}_{pot} avoiding the dispersion of solitons, caused by the kinetic term

$$\mathcal{L} = \mathcal{L}_{kin} + \mathcal{L}_{pot}. \quad (3.17)$$

According to [22] and adapted to MTF, using definition (3.2) of the field strength tensor $*F_{\mu\nu KM}$, the free Lagrangian is

$$\mathcal{L}_{kin} = \frac{1}{4\mu_0} *F_{\mu\nu KM} *F_{KM}^{\mu\nu} = \frac{1}{2} \left[\frac{1}{\mu_0} B_{iP} B_P^i - \epsilon_0 E_{iP} E_P^i \right] \quad (3.18)$$

with the magnetic field B_{iP} as well as the electric field E_{iP} . Eq. (3.18) can be expressed with the curvature tensor $R_{\mu\nu KM}$

$$\mathcal{L}_{kin} = \frac{\alpha_f \hbar c}{4\pi} \frac{1}{4} R_{\mu\nu KM} R_{KM}^{\mu\nu} \quad (3.19)$$

Regarding the electric field energy Eq. (3.16), respectively the kinetic Lagrangian (3.19), it is not possible to keep the soliton stabilized. This can be

seen easily by changing the scale for the contour function $\alpha(r)$. If one scales $r \rightarrow \lambda r$ with scaling factor $\lambda > 1$, then the field energy H_e will decrease by λ^{-1} .

$$r \longrightarrow \lambda r \quad \Longrightarrow \quad H_e \longrightarrow \lambda^{-1} H_e$$

That means the soliton tries to minimize its energy by dissolving and therefore dissolves completely. Hence there has to be introduced a potential energy, which preserves soliton's shape and structure² in Minkovski space.

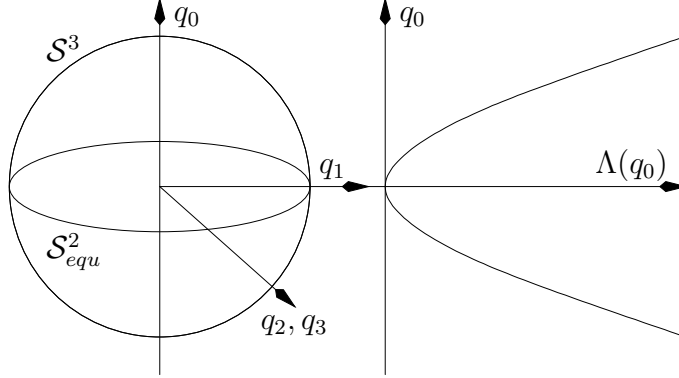


Figure 3.2: Potential term $\Lambda(q_0)$ of Lagrangian density of MTF with minimum at equatorial $\mathcal{S}_{\text{equ}}^2$ on a sphere \mathcal{S}^3 [14], [15].

So, the second part of Lagrangian density consists of the following general form

$$\mathcal{L}_{\text{pot}} = -\mathcal{H}_{\text{pot}} = -\frac{\alpha_f \hbar c}{4\pi} \Lambda(q_0) \quad (3.20)$$

with

$$\Lambda(q_0) = \frac{q_0^{2m}}{r_0^4} \quad \text{and} \quad m \in \mathbb{Z}^+ . \quad (3.21)$$

To keep the potential energy finite, \mathcal{H}_{pot} has to converge at infinity fast enough to zero. This requests even powers $q_0^{2m} = \cos^{2m} \alpha$. The free parameter r_0 is a type of unit length, describing the size of soliton centre. Also based on dimensional reasons $\Lambda(q_0)$ in Eq. (3.20) has to be of dimension $\text{length}^{-4} [m^{-4}]$. Such an energy term H_{pot} is scaling with λ^3 and stabilizes the soliton

$$r \longrightarrow \lambda r \quad \Longrightarrow \quad H_{\text{pot}} \longrightarrow \lambda^3 H_{\text{pot}} .$$

Therefore, the factor q_0 should vanish everywhere except around the soliton centre. This behaviour is supported by the choice of $\Lambda(q_0)$, see Fig. 3.2.

Consequently, the total Lagrangian density reads

$$\mathcal{L}_{MTF} = -\frac{\alpha_f \hbar c}{4\pi} \left(\frac{1}{4} R_{\mu\nu KM} R^{\mu\nu}_{KM} + \frac{q_0^{2m}}{r_0^4} \right) . \quad (3.22)$$

²In sine-Gordon model, the gravitational force keeps the soliton in shape.

3.2.1 Solution of soliton monopole

The variation of the Lagrangian function (3.22) produces the equation of motion for soliton monopoles. A derivation is shown in appendix A

$$q_K \frac{d\Lambda}{dq_0} + \partial_\mu (\varepsilon_{KLM} \Gamma_{\nu L} R_M^{\mu\nu}) = 0. \quad (3.23)$$

Inserting in Eq. (3.19) as well in Eq. (3.22), the definition (3.5) and Eq. (3.14), the variation for $\alpha = \alpha(\rho)$ with the dimensionless variable $\rho = \frac{r}{r_0}$ leads to a non linear differential equation of second order for the radial coordinate.

$$\partial_\rho^2 \cos^2 \alpha + \frac{1}{\rho^2} (1 - \cos^2 \alpha) \cos \alpha - m\rho^2 \cos^{2m-1} \alpha = 0. \quad (3.24)$$

In case of $m = 3$ the result for minimal energy and winding number $w_s = 1$ can be calculated algebraically. Eq. (3.24) can be solved by

$$\alpha(\rho) = \arctan \rho. \quad (3.25)$$

Inserting the above expression for $\alpha(\rho)$ in Eqs. (3.16) and (3.20), we get the total energy functional for the symmetric hedgehog ansatz

$$H = H_e + H_{\text{pot}} = \frac{\alpha_f \hbar c}{r_0} \int_0^\infty d\rho \left[\frac{\sin^4 \alpha}{2\rho^2} + (\partial_\rho \cos \alpha)^2 + \rho^2 \cos^{2m} \alpha \right]. \quad (3.26)$$

Using

$$\begin{aligned} \sin \alpha(\rho) &= \sin \arctan(\rho) = \frac{\rho}{\sqrt{1 + \rho^2}} \\ \cos \alpha(\rho) &= \cos \arctan(\rho) = \frac{1}{\sqrt{1 + \rho^2}} \end{aligned} \quad (3.27)$$

for the inverse trigonometric functions and inserting in the total energy functional (3.26) one gets

$$H = \frac{\alpha_f \hbar c}{r_0} \int_0^\infty d\rho \left[\frac{\rho^2}{2(1 + \rho^2)^2} + \frac{\rho^2}{(1 + \rho^2)^3} + \frac{\rho^2}{(1 + \rho^2)^3} \right]. \quad (3.28)$$

The three different contributions result from the radial electric field, the tangential electric field and the potential energy, respectively. The above integration³, Eq. (3.28), leads to the total energy H

$$H = \frac{\alpha_f \hbar c \pi}{r_0} \frac{1}{4}. \quad (3.29)$$

³The integration get

$$\begin{aligned} \int_0^\infty d\rho \frac{\rho^2}{2(1 + \rho^2)^2} &= \frac{1}{4} \left(\arctan \rho - \frac{\rho}{1 + \rho^2} \right) \Big|_0^\infty = \frac{1}{4} \frac{\pi}{2}, \\ \int_0^\infty d\rho \frac{\rho^2}{(1 + \rho^2)^3} &= \frac{1}{8} \left(\arctan \rho - \frac{\rho(1 - \rho^2)}{(1 + \rho^2)^2} \right) \Big|_0^\infty = \frac{1}{8} \frac{\pi}{2} \end{aligned}$$

Comparing the above result with the rest energy of electron/positron $E_{e^\pm} = m_e c^2 = 0.511 \text{ MeV}$, we obtain a soliton radius $r_0 = 2.21 \text{ fm}$. This value is close to the classical electron radius r_{e^-} , which multiplies the reduced Compton wavelength $\bar{\lambda} = \frac{\hbar}{m_e c}$ by Sommerfelds fine structure constant α_f

$$r_{e^-} = \frac{\alpha_f \hbar c}{m_e c^2} = \alpha_f \frac{\hbar}{m_e c} = 2.82 \text{ fm}. \quad (3.30)$$

3.3 Stable soliton configuration

In section 3.1 we have already mentioned the topology charge \mathcal{Q} and the number of windings w_s . Both quantum numbers are scalar quantities and do not change their values under rotations in colour space. Two different configurations in colour space, but both with same quantum numbers ($\mathcal{Q} = 1/2$, $w_s = 1$), are illustrated in Fig. 3.3. The difference refers to a rotation around the 3-axis by an angle π . In this figure the soliton field $Q(x^\mu)$ is displayed by imaginary part $q_K = n_K \sin \alpha$. These rotated configurations

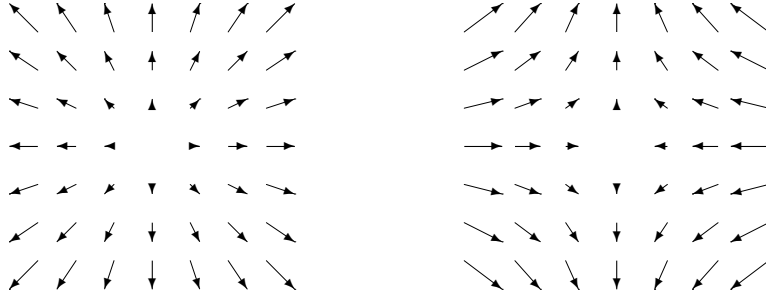


Figure 3.3: The imaginary part $q_K = n_K \sin \alpha$ of a negatively charged electric monopole is displayed in the hedgehog approach. The left figure is characterised by $n_K = \frac{r_K}{r}$ and the right side by $n_K = (-\frac{x}{r}, -\frac{y}{r}, \frac{z}{r})$. Both soliton fields are equivalent, just differing by a global rotation by π around the 3-axis in colour space.

have the same topological properties as the originals.

Further stable configurations, see table 3.1, with different topology we can get by *parity transformations* Π_n and *center transformations* z , respectively

$$Q \mapsto Q' = \Pi_n Q, \quad Q \mapsto Q' = zQ.$$

A *parity-transformation* changes the algebraic sign of $n_K \mapsto -n_K$. That means, the soliton field $Q = e^{-i\alpha\sigma_K n_K}$ is mapped to its adjoint, $Q \mapsto Q^\dagger$. By

considering Eq. (3.7) and due to $n_K [\varepsilon_{KLM} \partial_\partial n_L \partial_\varphi n_M]$, the winding number w_s changes its sign. Similarly, the topological charge \mathcal{Q} changes sign.

Generalising Eq. (3.8), we define the *topological current* k^μ

$$k^\mu = \frac{1}{12\pi^2} \varepsilon^{\mu\nu\rho\sigma} \Gamma_{\nu K} [\varepsilon_{KLM} \Gamma_{\rho L} \Gamma_{\sigma M}] \quad (3.31)$$

with the antisymmetric 4-Tensor $\varepsilon^{0123} = 1$. The topological charge \mathcal{Q} of Eq. (3.8) can therefore be expressed by

$$\mathcal{Q} = \int d^3r k^0(x^\mu). \quad (3.32)$$

Rewriting the topological current⁴ (3.31) by using the soliton field Q ,

$$k^\mu = \frac{1}{24\pi^2} \varepsilon^{\mu\nu\rho\sigma} \text{Tr} \left[\partial_\nu Q Q^\dagger \partial_\rho Q Q^\dagger \partial_\sigma Q Q^\dagger \right] \quad (3.33)$$

and applying the parity-transformation Π_n , we get

$$\begin{aligned} k^\mu \mapsto k'^\mu &= \Pi_n k^\mu = \frac{1}{24\pi^2} \varepsilon^{\mu\nu\rho\sigma} \Pi_n \text{Tr} \left[\partial_\nu Q Q^\dagger \partial_\rho Q Q^\dagger \partial_\sigma Q Q^\dagger \right] \\ &= \frac{1}{24\pi^2} \varepsilon^{\mu\nu\rho\sigma} \text{Tr} \left[\underbrace{\partial_\nu Q^\dagger Q}_{-\partial_\nu Q Q^\dagger} \underbrace{\partial_\rho Q^\dagger Q}_{-\partial_\rho Q Q^\dagger} \underbrace{\partial_\sigma Q^\dagger Q}_{-\partial_\sigma Q Q^\dagger} \right] \\ &= -\frac{1}{24\pi^2} \varepsilon^{\mu\nu\rho\sigma} \text{Tr} \left[\partial_\nu Q Q^\dagger \partial_\rho Q Q^\dagger \partial_\sigma Q Q^\dagger \right] = -k^\mu \end{aligned} \quad (3.34)$$

From Eq. (3.34) we see that the topological current k^μ , as well as the topological charge \mathcal{Q} change their sign.

The *centre transformation* $Q \mapsto Q' = zQ$ can be performed with $z = e^{i\pi\sigma_3}$. This center transformation in color space maps $n_K \mapsto -n_K$ and $\alpha \mapsto \pi - \alpha$. Hence, the product $\partial_\mu Q Q^\dagger$ and according to Eq. (2.81) the affine connection $\Gamma_{\mu K}$ do not change their sign. Therefore the topological charge \mathcal{Q} remains invariant under this transformation. However, the number of windings w_s gets a sign opposite to Eq. (3.7). A summary of interesting transformations is shown in table 3.1.

Characteristic soliton field configurations are shown in the bottom row of table 3.1. The arrows display the imaginary part of the soliton field $\Im Q(x^\mu) = q_K = n_K \sin \alpha$. From the identity $\frac{1}{2} \text{Tr} [Q Q^\dagger] = q_0^2 + q_K q_K = 1$ the real part

⁴Using the definition (3.31) of the topological current k^μ with $\text{Tr} [\sigma_K \sigma_L \sigma_M] = 2i\varepsilon_{KLM}$ as well as $\partial_\mu Q Q^\dagger + Q \partial_\mu Q^\dagger = 0$ we obtain Eq. (3.33)

$$\begin{aligned} k^\mu &= \frac{1}{12\pi^2} \varepsilon^{\mu\nu\rho\sigma} \Gamma_{\nu K} [\varepsilon_{KLM} \Gamma_{\rho L} \Gamma_{\sigma M}] = \frac{1}{24\pi^2} \varepsilon^{\mu\nu\rho\sigma} \text{Tr} [(i\sigma_K \Gamma_{\nu K})(i\sigma_L \Gamma_{\rho L})(i\sigma_M \Gamma_{\sigma M})] \\ &= \frac{1}{24\pi^2} \varepsilon^{\mu\nu\rho\sigma} \text{Tr} \left[\partial_\nu Q Q^\dagger \partial_\rho Q Q^\dagger \partial_\sigma Q Q^\dagger \right] = -\frac{1}{24\pi^2} \varepsilon^{\mu\nu\rho\sigma} \text{Tr} \left[Q \partial_\nu Q^\dagger Q \partial_\rho Q^\dagger Q \partial_\sigma Q^\dagger \right] \end{aligned}$$

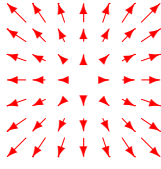
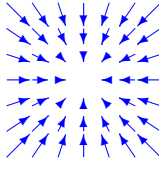
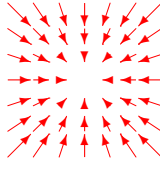
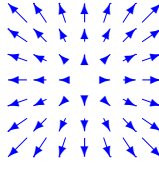
parameter	1	z	Π_n	$z\Pi_n$
n_K	r_K/r	$-r_K/r$	$-r_K/r$	r_K/r
q_0	≥ 0	≤ 0	≥ 0	≤ 0
w_s	1	-1	-1	1
$2\mathcal{Q}$	1	1	-1	-1
diagram				

Table 3.1: Short summary of different configurations of the soliton field Q under parity-transformation Π_n , center-transformation z and their product $z\Pi_n$. The effects of these transformations on n_K , q_0 , number of windings w_s and topological charge \mathcal{Q} are quoted. The figures display the imaginary part $q_K = n_K \sin \alpha$ of the hedgehog approach. Blue (dotted) vectors indicate negative $q_0 \leq 0$.

of $\Re Q = q_0 = \cos \alpha$ can be determined up to a sign. To indicate the sign of q_0 in the figure we choose different shafts of the arrows – red full lines indicate positive sign and blue (dotted) lines mark negative values of $-1 \leq q_0 \leq 0$, respectively. The length of vectors at the figures' borders is one and effectively both vector types become equal, $\alpha = \pi/2$, consequently $q_0 = 0$ or in layman's terms $\leftarrow = \leftarrow\text{-}$.

From the diagrams in table 3.1 we can read off the winding number w_s by the direction of vectors far away⁵ from the soliton center. Hedgehog solutions with vectors in outward direction have a positive integer $w_s > 0$, vectors with inward directions have negative integer windings $w_s < 0$.

Traversing the soliton center we read from the rotational matrices Q , that the local coordinate system in color space rotates by 2π around the direction of this motion. The configurations with topological charge $+1$, see table 3.1, correspond to right-handed rotations, correspondingly $\mathcal{Q} = -1$ to left-handed rotations. The four $\mathbf{SU}(2)$ -configurations of table 3.1 belong to different homotopy classes and therefore they can not be converted into each other by continuous deformations. The homotopy classes are classified by the topological quantum numbers \mathcal{Q} and w_s . Table 3.2 displays the left- and right-handed rotation of the local coordinate system, distinguished by the positive or neg-

⁵Actually, the number of windings w_s for a single soliton is measured integrating over the surface of a sphere \mathcal{S}^2 with radius $r \mapsto \infty$ in the *electrodynamic limit*. That implies $\alpha \mapsto \pi/2$ and $q_0 = 0$.

	$2\mathcal{Q}$	$w_s = 1$	$w_s = -1$
R	1	$\leftarrow \leftarrow \rightarrow \rightarrow$	$\rightarrow \rightarrow \leftarrow \leftarrow$
L	-1	$\leftarrow \leftarrow \rightarrow \rightarrow$	$\rightarrow \rightarrow \leftarrow \leftarrow$

Table 3.2: Four stable soliton configurations are shown for right-handed (clockwise) rotation R and for left-handed (counterclockwise) rotation L. Like in the preceding table 3.1, red / blue coloured vectors denote positive $q_0 \geq 0$ / negative $q_0 \leq 0$.

ative topological quantum number \mathcal{Q} .

3.4 Dipole soliton configuration

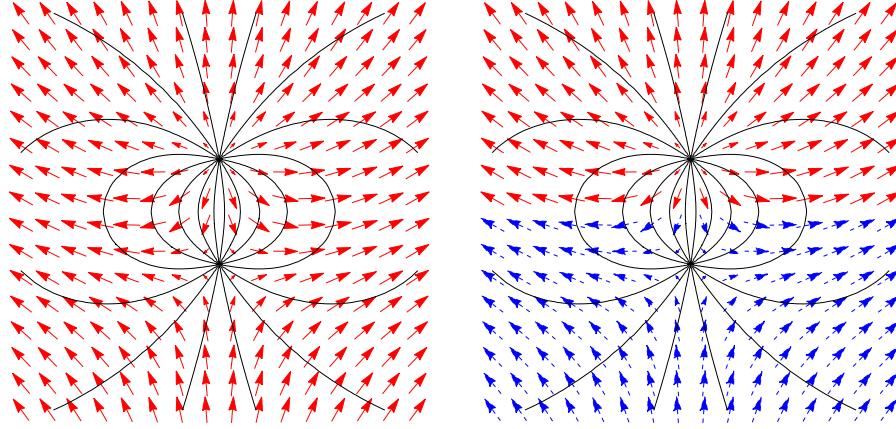
We want to construct configurations of two interacting solitons. Due to the interaction of solitons such configurations are not stable. In order to produce them with a minimization procedure we have to fix the centers of the monopoles. In the previous sections, we have already discussed stable monopole configurations with the hedgehog ansatz. Now, let us use these configurations and arrange the monopoles along the z -direction in a distance $d = 2a$ and compute the total energy of such a configuration.

From table 3.1 we conclude that within an $\mathbf{SU}(2)$ description there are nine different topological possibilities to combine two monopoles: Since topological charges are additive, $\mathcal{Q}_{dipole} = \mathcal{Q}_1 + \mathcal{Q}_2$, we obtain $\mathcal{Q}_{dipole} \in \{0, \pm 1\}$. Similar, the total number of windings w_s gets values $w_s = 0$ or $w_s \pm 2$.

In our $\mathbf{SO}(3)$ description dipole configurations with total charge $Q_{el} = -2e_0$ or $Q_{el} = 2e_0$ are physically distinguishable, but configurations with topological quantum number $\mathcal{Q}_{dipole} = \pm 1$ are not. This characteristic property is expressed in Eq. (3.10) by the absolute value $|\mathcal{Q}|$. This value does not depend whether a monopole resides in the northern $q_0 \geq 0$ or in the southern hemisphere $q_0 \leq 0$ of \mathcal{S}^3 .

However, without interactions with other charged particles, the sign of charges does not matter. Therefore, restricting ourselves to the analysis of negatively charged solitons will be sufficient.

Thus, four interesting dipole configurations are left – two of them feel attractive ($Q_{el} = 0$) and two repulsive forces ($Q_{el} = -2e_0$), each with spin $s = 0$ or $s = 1$. An example of a dipole configuration with attracting forces, that means with opposite unit charges $e^- - e^+$, is shown in the Figures 3.4a and 3.4b. These dipoles, consisting of two solitons, differ in topological quantum number \mathcal{Q} and consequently in total spin s_{tot} . Figure 3.4a corresponds to an attractive two soliton configuration with total spin $s_{tot} = 0$ and 3.4b to total spin $s_{tot} = 1$. The soliton fields are illustrated by coloured vectors, using the same style as described in table 3.1. Lengths and directions of vectors



(a) topological quantum numbers $w_s = \mathcal{Q} = 0$, as follows total charge $Q_{dipole} = 0$, total spin $s_{tot} = 0$.
 (b) topological quantum numbers $w_s = 0$, $\mathcal{Q} = 2$, as follows total charge $Q_{dipole} = 0$, total spin $s_{tot} = 1$.

Figure 3.4: Schematic presentation taken from [15] of two solitons with opposite unit charges $e^- - e^+$. Both figures show a dipole configuration with attracting forces. The configuration is arranged symmetrically around z -direction. Vectors illustrate the imaginary soliton Q -field with $q_K = n_K \sin \alpha$. Using the same colours as in table 3.1 for vectors, red stands for a positive $q_0 = \cos \alpha \geq 0$ and blue for negative $q_0 \leq 0$, respectively. Lines of the electric field are plotted in black.

represent the imaginary part of the soliton field $q_K = n_K \sin \alpha$. Red coloured vectors indicate positive $q_0 \geq 0$, in contrast blue vectors negative $q_0 \leq 0$.

To evaluate exact solutions of dipole configurations, we have to solve the equation of motion (3.23), which is not yet solvable by algebraic methods. As already mentioned, static dipole configurations of solitons are assembled by two single soliton solutions with $m = 3$ and their soliton center are \vec{R}_+ and \vec{R}_- , respectively. That is

$$\alpha(r) = \arctan \frac{r}{r_0} \quad \text{and} \quad \vec{R}_+ = (0, 0, +a)^T, \quad \vec{R}_- = (0, 0, -a)^T. \quad (3.35)$$

Near the soliton center, the approximation uses the electric field \vec{E} of the single monopole solution and only if the distance d of both solitons becomes equivalent $d \approx 2r_0$ or even smaller $d < r_0$, then the interaction between the solitons will be considered and approximated. Regarding the deviation of the known electric dipole field, we will use the ansatz

$$\alpha(\vec{r}) = \arctan \frac{\bar{r}}{r_0} \quad \text{with} \quad \frac{1}{\bar{r}} = \left| \frac{1}{r_-} \pm \frac{1}{r_+} \right|, \quad r_{\pm} = |\vec{r} - \vec{R}_{\pm}|. \quad (3.36)$$

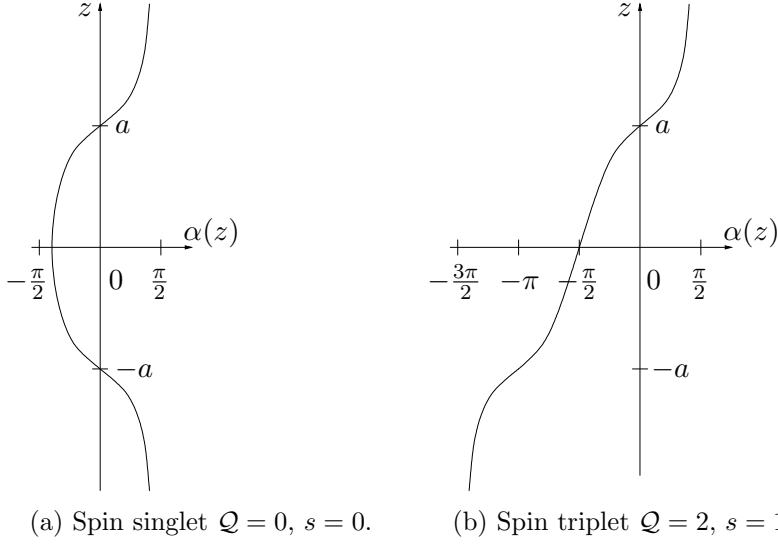


Figure 3.5: Schematic profile of the α -contour-function of two solitons with opposite charges $e^- - e^+$ in z -direction (positronium). The configuration of the soliton field $Q(x^\mu)$ is assumed $Q = \cos \alpha + i\sigma_3 \sin \alpha$. Topological quantum numbers of the left/right-handed picture correspond with those from figures 3.4a/3.4b.

The contour-function $\alpha(\vec{r})$ is shown in Fig. 3.5, permitting a wider interval with negative values. To provide distinct values of the soliton field $Q(x^\mu)$, we restrict n_K to the northern hemisphere by limiting $n_3 > 0$. Differences between both shapes of curves lead to different total energies of both configurations. A combined configuration with $|2\mathcal{Q}| = s = 0$ does not cover the complete sphere \mathcal{S}^3 and has therefore lower energy than the configuration with $|2\mathcal{Q}| = s = 1$, covering the total sphere \mathcal{S}^3 . Starting from a large distance $d = 2a$ of the soliton centers, reducing this distance leads to decreasing curvature and consequently total energy. This agrees with Coulomb's law for a dipole. For short distances $d \lesssim 2r_0$ a deviation from the Coulomb field of point charges is observed. This reminds at the *running coupling constant* α_f , well known from QED.

The solitons, illustrated on the left hand side of the Fig. 3.4a and Fig. 3.5a have the same quantum numbers as the vacuum, $|2\mathcal{Q}| = s = 0$ and $w_s = 0$, therefore they can annihilate. With decreasing distance between the soliton pair the torsions/windings are compensated. This demonstrates that particle–antiparticle annihilation can take place already at the classical level. Figures 3.4b and 3.5b show solitons with total topological quantum number $\mathcal{Q}_{\text{tot}} = 1$. For this configuration particle–annihilation is not so simply possible. This state corresponds to the triplet-state of *positronium*, which is known to

decay by emission of three photons.

3.4.1 Electric field of a dipole

In the *electrodynamic limit* the electric force lines follow lines with constant $n_K = \text{const.}$ Due to the cylindrical symmetry of the dipole the common soliton field is expected to be cylindrical symmetric. For cylindrical coordinates ρ, φ, z it is convenient to chose the z -axis through both soliton centers. We parametrize the n_K -field of two attracting charges by⁶

$$n_K(\vec{r}) = \begin{pmatrix} \sin \theta(\vec{r}) \cos \phi(\vec{r}) \\ \sin \theta(\vec{r}) \sin \phi(\vec{r}) \\ \cos \theta(\vec{r}) \end{pmatrix} \quad (3.37)$$

with angles $\{\theta, \phi\} \in \mathcal{S}^2$ and

$$\cos \theta(\vec{r}) = 1 + \frac{z_-}{\sqrt{z_-^2 + \rho^2}} - \frac{z_+}{\sqrt{z_+^2 + \rho^2}} \quad \text{and} \quad \phi = \varphi. \quad (3.38)$$

Furthermore, using the shortcuts

$$z_{\pm} = z \pm a, \quad r_{\pm} = \sqrt{z_{\pm}^2 + \rho^2}, \quad (3.39)$$

we get for the electric field components of a dipole

$$\begin{aligned} E_{\rho} &= \frac{e_0}{4\pi\epsilon_0} \left[\frac{\rho}{r_+^3} - \frac{\rho}{r_-^3} \right] \\ E_{\varphi} &= 0 \\ E_z &= \frac{e_0}{4\pi\epsilon_0} \left[\frac{z_+}{r_+^3} - \frac{z_-}{r_-^3} \right]. \end{aligned} \quad (3.40)$$

3.4.2 Cylindrical symmetric configuration

If we put the 3-axis through both center of a static soliton – anti-soliton pair, the configuration is axially symmetric around the 3-axis. It its convenient to describe the soliton field in cylindrical coordinates too. The following ansatz is used for the cylindrical symmetric soliton field $Q = Q(r, \varphi, z)$

$$Q(r, \varphi, z) = q_0(r, z) - i\sigma_K q_K(r, \varphi, z) \quad (3.41)$$

with

$$q_K(r, \varphi, z) = \begin{pmatrix} q_r(r, z) \cos \varphi \\ q_r(r, z) \sin \varphi \\ q_z(r, z) \end{pmatrix}. \quad (3.42)$$

⁶The derivation of the n_K -field is described in detail in appendix B.

Requiring the soliton field⁷ $Q(x^\mu) \in \mathbb{H}_{unit}$, therefore the norm of Q is

$$\|Q\| = q_0^2 + q_K q_K = q_0^2 + q_r^2 + q_z^2 = 1. \quad (3.43)$$

According to Eq. (2.81) and explicitly (3.12), the affine connection Γ_{sK} of the soliton field Q is in general

$$\Gamma_{sK} = q_0 \partial_s q_K - q_K \partial_s q_0 + \varepsilon_{KLM} q_L \partial_s q_M. \quad (3.44)$$

Using the vanishing derivatives $\partial_\varphi q_r = \partial_\varphi q_z = \partial_r \varphi = \partial_z \varphi = 0$ in cylindrical coordinates⁸ we get

$$\begin{aligned} \Gamma_{rK} &= \begin{pmatrix} [q_r \partial_r q_z - q_z \partial_r q_r] \sin \varphi + [q_0 \partial_r q_r - q_r \partial_r q_0] \cos \varphi \\ -[q_r \partial_r q_z - q_z \partial_r q_r] \cos \varphi + [q_0 \partial_r q_r - q_r \partial_r q_0] \sin \varphi \\ q_0 \partial_r q_z - q_z \partial_r q_0 \end{pmatrix}, \\ \Gamma_{\varphi K} &= q_r \begin{pmatrix} -q_0 \sin \varphi - q_z \cos \varphi \\ q_0 \cos \varphi - q_z \sin \varphi \\ q_r \end{pmatrix}, \\ \Gamma_{zK} &= \begin{pmatrix} [q_r \partial_z q_z - q_z \partial_z q_r] \sin \varphi + [q_0 \partial_z q_r - q_r \partial_z q_0] \cos \varphi \\ -[q_r \partial_z q_z - q_z \partial_z q_r] \cos \varphi + [q_0 \partial_z q_r - q_r \partial_z q_0] \sin \varphi \\ q_0 \partial_z q_z - q_z \partial_z q_0 \end{pmatrix}. \end{aligned} \quad (3.45)$$

Similarly, using the *Maurer-Cartan* Eq. (2.96) the curvature tensor R_{stKM} , defined in Eq. (2.88) evaluates to

$$R_{stKM} = T_{KML} R_{stL} = T_{KML} \varepsilon_{LNP} \Gamma_{sN} \Gamma_{tP} \quad (3.46)$$

⁷The set of unit quaternion is

$$\mathbb{H}_{unit} = \{Q \in \mathbb{H} \mid \|Q\| = 1\}.$$

⁸The derivation of Eq. (3.45) is using the following identities

$$\begin{aligned} \partial_s q_K &= \begin{pmatrix} \partial_s q_r \cos \varphi - q_r \sin \varphi \partial_s \varphi \\ \partial_s q_r \sin \varphi + q_r \cos \varphi \partial_s \varphi \\ \partial_s q_z \end{pmatrix}, \\ \varepsilon_{KLM} q_L \partial_s q_M &= \begin{pmatrix} [q_r \partial_s q_z - q_z \partial_s q_r] \sin \varphi - q_z q_r \cos \varphi \partial_s \varphi \\ -[q_r \partial_s q_z - q_z \partial_s q_r] \cos \varphi - q_z q_r \sin \varphi \partial_s \varphi \\ q_r^2 \partial_s \varphi \end{pmatrix}. \end{aligned}$$

Further we derive from Eq. (3.43)

$$-q_0 \partial_s q_0 = q_r \partial_s q_r + q_z \partial_s q_z \quad \text{and} \quad q_0 = \sqrt{1 - q_r^2 - q_z^2}.$$

with the generators $T_L = T_{L(KM)}$ of the Lie-group $\mathbf{SU}(2)$, see Eqs. (2.47) and (2.83). Displaying Eq. (3.46) in cylindrical coordinates (r, φ, z) , we get for $R_{stL} = (R_{23L}, R_{31L}, R_{12L})^T = (R_{\varphi zL}, R_{zrL}, R_{r\varphi L})^T$ with

$$R_{\varphi zL} = q_r \begin{pmatrix} \partial_z q_0 \sin \varphi + \partial_z q_z \cos \varphi \\ -\partial_z q_0 \cos \varphi + \partial_z q_z \sin \varphi \\ -\partial_z q_r \end{pmatrix}, \quad (3.47)$$

$$R_{zrL} = \frac{\partial_r q_r \partial_z q_z - \partial_z q_r \partial_r q_z}{q_0} \begin{pmatrix} -q_0 \sin \varphi - q_z \cos \varphi \\ q_0 \cos \varphi - q_z \sin \varphi \\ q_r \end{pmatrix}, \quad (3.48)$$

$$R_{r\varphi L} = q_r \begin{pmatrix} -\partial_r q_0 \sin \varphi - \partial_r q_z \cos \varphi \\ \partial_r q_0 \cos \varphi - \partial_r q_z \sin \varphi \\ \partial_r q_r \end{pmatrix}. \quad (3.49)$$

We need the squares $R_{stL} R_{stL}$ for the calculation of the energy- or Lagrange densities

$$R_{\varphi zL} \cdot R_{\varphi zL} = q_r^2 \left[(\partial_z q_0)^2 + (\partial_z q_r)^2 + (\partial_z q_z)^2 \right], \quad (3.50)$$

$$R_{rzL} \cdot R_{rzL} = \frac{1}{q_0^2} \left(\partial_r q_r \partial_z q_z - \partial_z q_r \partial_r q_z \right)^2, \quad (3.51)$$

$$R_{r\varphi L} \cdot R_{r\varphi L} = q_r^2 \left[(\partial_r q_0)^2 + (\partial_r q_r)^2 + (\partial_r q_z)^2 \right]. \quad (3.52)$$

For the sake of completeness, we display explicitly the electric field components E_{iL} , as already specified in Eq. (3.2)

$$\begin{aligned} E_{rL} &= -\frac{e_0}{4\pi\epsilon_0} \frac{1}{l_\phi l_z} R_{\varphi zL}, \\ E_{\varphi L} &= \frac{e_0}{4\pi\epsilon_0} \frac{1}{l_r l_z} R_{rzL}, \\ E_{zL} &= -\frac{e_0}{4\pi\epsilon_0} \frac{1}{l_r l_\phi} R_{r\varphi L} \end{aligned} \quad (3.53)$$

with the length scales of the cylindrical basis system $l_r = 1, l_\varphi = r, l_z = 1$.

As already mentioned in the beginning of this section 3.4, we want to evaluate the total energy density \mathcal{H} . Based on equations (3.50) – (3.53), the curvature energy density \mathcal{H}_c of the soliton field Q is

$$\begin{aligned} \mathcal{H}_c &= \frac{1}{2} \epsilon_0 |E_{iL}|^2 = \frac{1}{2} \epsilon_0 \left(E_{rL}^2 + E_{\varphi L}^2 + E_{zL}^2 \right) \\ &= \frac{\epsilon_0}{2} \left(\frac{e_0}{4\pi\epsilon_0} \right)^2 \frac{1}{r^2} \left(R_{\varphi zL} \cdot R_{\varphi zL} + r^2 R_{rzL} \cdot R_{rzL} + R_{r\varphi L} \cdot R_{r\varphi L} \right) \end{aligned} \quad (3.54)$$

At last, with Eqs. (3.50) – (3.52) we express the desired energy density \mathcal{H}_c in terms of the *fine-structure constant* α_f ⁹

$$\begin{aligned} \mathcal{H}_c = & \frac{1}{2} \frac{\alpha_f \hbar c}{4\pi} \frac{1}{r^2} \left[q_r^2 \left[(\partial_z q_0)^2 + (\partial_z q_r)^2 + (\partial_z q_z)^2 \right] \right. \\ & + \frac{r^2}{q_0^2} (\partial_r q_r \partial_z q_z - \partial_z q_r \partial_r q_z)^2 \\ & \left. + q_r^2 \left[(\partial_r q_0)^2 + (\partial_r q_r)^2 + (\partial_r q_z)^2 \right] \right]. \end{aligned} \quad (3.55)$$

⁹The definition of *fine-structure constant* α_f reads

$$\alpha_f = \frac{e_0^2}{4\pi\epsilon_0\hbar c}, \quad \text{that is} \quad \frac{\hbar c\alpha_f}{e_0} = \frac{e_0}{4\pi\epsilon_0}.$$

Chapter 4

Lattice computation

Based on earlier studies of Joachim Wabnig [16] and Josef Resch [17], we have decided to reinvestigate soliton-pairs by a lattice computation. For this purpose we have recycled some of the ideas and workflow of Wabnig's C-procedures. However, except the initialisation part and Powell's minimization routine from Numerical Recipes [18], all other routines were written completely new.

To solve a soliton-scattering problem numerically, one would have to use a four dimensional lattice, consisting of three space- and one time-direction. Here, we consider static snapshots of the soliton pair at different distances. Exploiting the cylindrical symmetry, the lattice can be reduced to two dimensions. Visualising a cross-section of the soliton pair at an arbitrary angle $\varphi = \varphi_0$, we put \vec{e}_r and \vec{e}_z in that plane. This allows us, to restrict the calculation to $R \cdot Z$ points, where R, Z are the numbers of lattice sites in the particular directions \vec{e}_r, \vec{e}_z . At each lattice site there is a soliton field $Q(r, z)$. We use the ansatz of section 3.4.2 for the soliton field Q . Due to Eqs. (3.41) and (3.42) and the normalisation (3.43), RAM¹ usage of only two double floating point variables $q_r(r, z)$ and $q_z(r, z)$ per lattice site is necessary.

The derivatives $\partial_i q_j$ are computed as differences between lattice sites. Using Eq. (3.55), we are able to evaluate the energy density $\mathcal{H}_c(r, z)$ for all lattice points. Integrating over the whole lattice by summing over the interim results, we get the total energy of the configuration as a function of the soliton field at each point. This energy function will be minimised by Powell's procedure. After each iteration step we recalculate the total energy of the configuration. This is some type of cooling procedure for the soliton field. If further iterations do not modify more than a chosen lower bound, the routine will stop. Assuming, a local minimisation level of the total energy of the configuration is reached.

¹Random Access Memory

4.1 Evaluating total energy

According to Eq. (3.55), we need in addition to q_j the derivatives $\partial_i q_j$. To evaluate their values at every lattice site, we consider the differences to neighbouring sites divided by the lattice constant a . In general, we have an arbitrary discrete function $f = f(x_i)$ with running parameter x_i in any of both directions, that means at

$$0 \leq \dots \leq x_{i-1} \leq x_i \leq \dots \quad \text{and} \quad 0 \leq i \leq N \quad \text{with} \quad i, N \in \mathbb{N}.$$

The derivative is approximated by the the left derivative

$$\frac{df}{dx_i} \approx \frac{\Delta f}{\Delta x_i} = \frac{f(x_i) - f(x_{i-1})}{\Delta x_i} = \frac{f(x_i) - f(x_{i-1})}{a} \quad (4.1)$$

with $\Delta x_i = x_i - x_{i-1} = a$. The right derivative is defined similarly

$$\frac{df}{dx_i} \approx \frac{\Delta f}{\Delta x_i} = \frac{f(x_{i+1}) - f(x_i)}{a}. \quad (4.2)$$

At the boundaries of the lattice we are only able to use neighboring points from one direction.

To get higher accuracy calculating the derivatives, we take both neighbouring points into account. For this purpose we consider the polynomial of grade two $g(x) = a_2 x^2 + a_1 x + a_0$ and determine the unknown constants a_2 , a_1 and a_0 from $f(x_{i-1})$, $f(x_i)$ and $f(x_{i+1})$. The derivative of $g(x)$ is given by

$$\frac{dg}{dx} = 2a_2 x + a_1.$$

This expression is a second order approximation to the derivative $\frac{df}{dx_i}$

$$\frac{df}{dx_i} \approx \frac{f(x_{i+1}) - f(x_{i-1}))}{2a}. \quad (4.3)$$

Enhancing the above concept by using five points – two neighbours to the left, to the right and the middle point – we fit a forth-grade polynomial to calculate the derivative at position x_i

$$\frac{df}{dx_i} \approx \frac{f(x_{i-2}) - 8f(x_{i-1}) + 8f(x_{i+1}) - f(x_{i+2}))}{12a}. \quad (4.4)$$

Evaluating derivatives, we always take the formula with the highest precision where possible into account. Only near the boundaries we have to reduce the number of points used.

4.1.1 Summation of total energy

The total energy H_{tot} is calculated by integration of the curvature energy density \mathcal{H}_c , defined in Eq. (3.19), and the potential energy density \mathcal{H}_{pot} from Eq. (3.20) over the complete volume, that is

$$H_{\text{tot}} = \int_V d^3x [\mathcal{H}_c + \mathcal{H}_{\text{pot}}] . \quad (4.5)$$

We want to compute Eq. (4.5) on the lattice. For this, we introduce coordinates in multiples of the lattice spacing a

$$r = a\bar{r} , \quad \varphi = \bar{\varphi} , \quad z = a\bar{z} . \quad (4.6)$$

That means, the parameters \bar{r} , $\bar{\varphi}$ and \bar{z} just number the lattice points. Substituting the above assignments (4.6) in the derivatives, we get

$$\partial_r q_K = \frac{1}{a} \frac{\partial q_K(r, z)}{\partial \bar{r}} = \frac{1}{a} \partial_{\bar{r}} q_K \equiv \frac{1}{a} \bar{\partial}_r q_K \quad \text{and} \quad \partial_z q_K = \frac{1}{a} \bar{\partial}_z q_K , \quad (4.7)$$

respectively. Furthermore the curvature R_{stL} will be replaced by

$$R_{stL} \equiv \frac{1}{a^2} \bar{R}_{stL} = \frac{1}{a^2} \varepsilon_{LMN} \bar{\Gamma}_{sM} \bar{\Gamma}_{tN} \quad (4.8)$$

with $\Gamma_{sK} \equiv \frac{1}{a} \bar{\Gamma}_{sK}$. Remembering the result of Eq. (3.55) and including the above statements, we obtain the curvature energy H_c

$$\begin{aligned} H_c &= \frac{1}{2} \frac{\alpha_f \hbar c}{4\pi} \int_V \underbrace{r dr d\varphi dz}_{a^3 \bar{r} d\bar{r} d\bar{\varphi} d\bar{z}} \frac{1}{r^2} (R_{\varphi z L}^2 + r^2 R_{zr L}^2 + R_{r\varphi L}^2) , \\ &= \frac{1}{2} \frac{\alpha_f \hbar c}{4\pi} \int_V a^3 \bar{r} d\bar{r} d\bar{\varphi} d\bar{z} \frac{1}{(a\bar{r})^2} \left(\frac{1}{a^2} \bar{R}_{\varphi z L}^2 + (a\bar{r})^2 \frac{1}{a^4} \bar{R}_{zr L}^2 + \frac{1}{a^2} \bar{R}_{r\varphi L}^2 \right) . \end{aligned}$$

Integration by $d\varphi$ gives a factor of 2π . After a lengthy calculation the curvature energy reads

$$\begin{aligned} H_c &= \frac{\alpha_f \hbar c}{4a} \left(\int \frac{d\bar{r} d\bar{z}}{\bar{r}} q_r^2 \underbrace{[(\bar{\partial}_r q_0)^2 + (\bar{\partial}_r q_r)^2 + (\bar{\partial}_r q_z)^2]}_{\tilde{\mathcal{H}}_1} + \right. \\ &\quad \left. + \int \bar{r} d\bar{r} d\bar{z} \frac{1}{q_0^2} \underbrace{(\bar{\partial}_r q_r \bar{\partial}_z q_z - \bar{\partial}_z q_r \bar{\partial}_r q_z)^2}_{\tilde{\mathcal{H}}_2} + \right. \\ &\quad \left. + \int \frac{d\bar{r} d\bar{z}}{\bar{r}} q_r^2 \underbrace{[(\bar{\partial}_z q_0)^2 + (\bar{\partial}_z q_r)^2 + (\bar{\partial}_z q_z)^2]}_{\tilde{\mathcal{H}}_3} \right) . \quad (4.9) \end{aligned}$$

Rearranging the terms and introducing the further shortcuts \mathcal{H}_i with $i = 1, 2, 3$, the result is

$$H_c = \frac{\alpha_f \hbar c}{a} \frac{1}{4} \underbrace{\left(\int d\bar{r} d\bar{z} \left[\frac{1}{\bar{r}} \bar{\mathcal{H}}_1 + \bar{r} \bar{\mathcal{H}}_2 + \frac{1}{\bar{r}} \bar{\mathcal{H}}_3 \right] \right)}_{\bar{H}_c} = \frac{\alpha_f \hbar c}{a} \bar{H}_c \quad (4.10)$$

As already mentioned in the beginning, to calculate potential energy H_{pot} of Eq. (4.5), we start with the definition of potential energy density of Eq. (3.20)

$$H_{\text{pot}} = \frac{\alpha_f \hbar c}{4\pi} \frac{1}{r_0^4} \int_V d^3x q_0^{2m}.$$

Again, assigning a pure number to the soliton radius $r_0 = a\bar{r}_0$, we get

$$\begin{aligned} H_{\text{pot}} &= \frac{\alpha_f \hbar c}{4\pi} \frac{1}{(a\bar{r}_0)^4} \underbrace{\int_{2\pi} d\bar{\varphi}}_{2\pi} \int a^3 \bar{r} d\bar{r} d\bar{z} q_0^{2m}, \\ &= \frac{\alpha_f \hbar c}{a} \frac{1}{2\bar{r}_0^4} \underbrace{\int d\bar{r} d\bar{z} \bar{r} q_0^{2m}}_{\bar{H}_{\text{pot}}} = \frac{\alpha_f \hbar c}{a} \bar{H}_{\text{pot}}. \end{aligned} \quad (4.11)$$

Thus, the total energy H_{tot} adds up to

$$H_{\text{tot}} = \frac{\alpha_f \hbar c}{a} \bar{H}_{\text{tot}} = \frac{\alpha_f \hbar c}{a} [\bar{H}_c + \bar{H}_{\text{pot}}]. \quad (4.12)$$

4.1.2 Energy contribution of a monopole outside the box

Since the lattice contains a finite volume of the total space only, we have to consider the remaining space and gather contributions of the energy outside the grid. Being far away from the soliton center we are using common electrodynamic equations for a localised charge. We want to calculate the total energy outside the lattice boundary. The electric potential Φ adapted for the lattice space in cylindrical coordinates is

$$\Phi = \frac{1}{4\pi\epsilon_0} \frac{q}{|\vec{r}|} = \frac{1}{4\pi\epsilon_0} \frac{q}{\sqrt{r^2 + z^2}} \quad (4.13)$$

with $q = e_0$. We obtain for the electrical field \vec{E}

$$\vec{E} = -\nabla\Phi = \frac{q}{4\pi\epsilon_0} \frac{\vec{r}}{r^3} = \frac{1}{4\pi\epsilon_0} \frac{q}{\sqrt{(r^2 + z^2)^3}} \begin{pmatrix} r \\ 0 \\ z \end{pmatrix}. \quad (4.14)$$

Now, calculating the energy outside of the cylindrical box, we have to determine the integral

$$H_{\text{out}} = \frac{\epsilon_0}{2} \int_{\text{out}} d^3x E_i E_i. \quad (4.15)$$

Due to the radial symmetry, the φ -integration is easily obtained $\int d\varphi = 2\pi$. Hence, there remains the integration in the r - z -plane. For a convenient calculation we divide this area in three sections

Section	r	z
I	$0 < r < \infty$	$-\infty < z < -Z$
II	$R < r < \infty$	$-Z < z < +Z$
III	$0 < r < \infty$	$Z < z < \infty$

where R, Z are the numbers of lattice points in the corresponding direction. Inserting Eq. (4.14) in the integral (4.15) we write

$$\begin{aligned} H_{\text{out}} &= \frac{\epsilon_0}{2} \frac{q^2}{(4\pi\epsilon_0)^2} \int \frac{r^2 + z^2}{(r^2 + z^2)^3} r dr d\varphi dz \\ &= \frac{\epsilon_0}{2} \frac{q^2}{(4\pi\epsilon_0)^2} 2\pi \int \frac{r dr dz}{(r^2 + z^2)^2}. \end{aligned}$$

Using the substitution $r^2 + z^2 = u$ and $du = 2r dr$ for the dr -integration, the above equation becomes

$$\begin{aligned} H_{\text{out}} &= \frac{2\pi\epsilon_0}{2} \frac{q^2}{(4\pi\epsilon_0)^2} \int \frac{du dz}{2u^2} = \frac{2\pi\epsilon_0}{2} \frac{q^2}{(4\pi\epsilon_0)^2} \left(-\frac{1}{2} \right) \int \frac{dz}{u(r, z)} \Big|_{I, II, III} \\ &= \frac{2\pi\epsilon_0}{4} \frac{q^2}{(4\pi\epsilon_0)^2} \left[\int_{-\infty}^{-Z} \frac{dz}{z^2} + \int_{-Z}^Z \frac{dz}{R^2 + z^2} + \int_Z^{\infty} \frac{dz}{z^2} \right]. \end{aligned}$$

For the dz -integration in the middle term we substitute $z/R = \tan \alpha$. Hence, for the integration variable dz we derive $dz/R = (1 + \tan^2 \alpha) d\alpha$. Solving the above definite integrals² and again replacing α , using the interval limits for z , that is

$$\begin{aligned} H_{\text{out}} &= \frac{\epsilon_0}{2} \frac{q^2}{(4\pi\epsilon_0)^2} \frac{2\pi}{2} \left[-\frac{1}{z} \Big|_{-\infty}^{-Z} + \frac{1}{R} \arctan \frac{z}{R} \Big|_{-Z}^Z - \frac{1}{z} \Big|_Z^{\infty} \right] \\ &= \frac{\epsilon_0}{2} \frac{q^2}{(4\pi\epsilon_0)^2} \frac{2\pi}{2} \left[\frac{2}{Z} + \frac{2}{R} \arctan \frac{Z}{R} \right]. \end{aligned} \tag{4.16}$$

²We use indefinite integral

$$\int \frac{dz}{R^2 + z^2} = \int \frac{1}{R^2} \frac{(1 + \tan^2 \alpha) R d\alpha}{1 + \tan^2 \alpha} = \frac{\alpha}{R} + C \text{ with } \tan \alpha = z/R.$$

Consequently with $R = a\bar{R}$ and $Z = a\bar{Z}$ the result is

$$\begin{aligned} H_{\text{out}} &= \frac{e_0^2}{4\pi\epsilon_0} \frac{2\pi\epsilon_0}{4\pi\epsilon_0} \frac{2}{4} \left[\frac{1}{a\bar{Z}} + \frac{1}{a\bar{R}} \arctan \frac{\bar{Z}}{\bar{R}} \right] \\ &= \frac{\alpha_f \hbar c}{a} \frac{1}{4} \underbrace{\left[\frac{1}{\bar{Z}} + \frac{1}{\bar{R}} \arctan \frac{\bar{Z}}{\bar{R}} \right]}_{\bar{H}_{\text{out}}} = \frac{\alpha_f \hbar c}{a} \bar{H}_{\text{out}} . \end{aligned} \quad (4.17)$$

4.1.3 Hartree atomic units

Comparing the computed energy \bar{H}_{tot} from lattice simulation just with one soliton to mass-energy equivalent of an electron $E = m_e c^2 = 511 \text{ keV}$, we are able to determine the lattice length a . Equalising both expressions, that is

$$m_e c^2 = \frac{\alpha_f \hbar c}{a} \bar{H}_{\text{tot}}$$

and solving for lattice space length a , we obtain

$$a = \frac{\alpha_f \hbar}{m_e c} \bar{H}_{\text{tot}} = \alpha_f^2 a_0 \bar{H}_{\text{tot}} \quad (4.18)$$

with *Bohr* radius³ $a_0 = \frac{\hbar}{m_e c \alpha_f}$. Now we are able to verify the quality of our model comparing the classical electron radius r_e with $r_0 = a\bar{r}_0$.

Doing the same calculation by using *Hartree atomic* units, we redefine the following units

$$e_0 = m_e = \hbar = c \alpha_f = 1 \quad \text{and} \quad c = 137,036 .$$

This setting provides as length unit the *Bohr* radii a_0 , the energy unit is the *Hartree energy*⁴ unit E_h

$$E_h = \frac{\hbar^2}{m_e a_0^2} = \frac{\hbar c \alpha_f}{a_0} = m_e (c \alpha_f)^2 .$$

Again, calculating the lattice constant a , equations (4.12) and (4.18) become in *Hartree* units

$$[H_{\text{tot}}]_H = \frac{1}{a} \bar{H}_{\text{tot}} = \frac{1}{a} [\bar{H}_c + \bar{H}_{\text{pot}}] , \quad (4.19)$$

$$[a]_H = \frac{\alpha_f}{c} \bar{H}_{\text{tot}} = \alpha_f^2 \bar{H}_{\text{tot}} . \quad (4.20)$$

³Bohr radius $a_0 = 5,292 \cdot 10^{-11} \text{ m}$

⁴Hartree energy $E_h = 4,35974434(19) \cdot 10^{-18} \text{ J} = 27,21138505(60) \text{ eV}$.

The result is given in multiples of a_0 . For example, using a lattice size of 61×30 the simulation of the energy (4.19) results in a value of $\bar{H}_{\text{tot}} \approx 0,26$. Therefore we get for the lattice constant a and for the soliton radius⁵ $r_0 = 3a$ the following values

$$\begin{aligned} [a]_H &= \frac{0,26}{137,036^2} a_0 = 1,38397 \cdot 10^{-5} a_0 \\ a &= 1,38397 \cdot 10^{-5} \cdot 0,5292 \cdot 10^{-10} \text{ m} = 0,732398 \text{ fm} \\ r_0 &= 3a = 2,1972 \cdot 10^{-15} \text{ m} = 2,1972 \text{ fm} \end{aligned}$$

Since, in section 3.2.1 we have already solved the field configuration of a monopole from Eq. (3.26) with $m = 3$ in an algebraic way, we can check the accuracy of the lattice simulation comparing the numerical result with the soliton radius $r_0 = 2.21$ fm. The results differ by a few percent, due to the presumable imperfect energy minimization caused by the program routines.

4.1.4 Energy Contribution of a dipole outside the box

As mentioned in section 4.1.2, we assume the validity of common electrodynamics outside the lattice volume. Hence, the electrodynamic limit at the lattice boundaries has to be valid. An essential precondition is the vanishing of the soliton potential $\Lambda(q_0)$, which implies $q_0 = 0$. Only the radial colour component in direction of n_K still contributes to the energy density. The total energy is calculated by integration over the total volume of the squared electric field E_{iL}^2 , see Eq. (4.15)

$$H_{\text{out}} = \frac{\epsilon_0}{2} \int_V d^3x E_{iL}^2. \quad (4.21)$$

In analogy to electrodynamics using Green's first identity

$$E_i^2 = (\nabla_i \Phi)^2 = \nabla_i (\Phi \nabla_i \Phi) - \Phi \Delta \Phi, \quad (4.22)$$

we rewrite Eq. (4.21) to

$$H_{\text{out}} = \frac{\epsilon_0}{2} \oint d^2 f_i \Phi \nabla_i \Phi = \frac{\epsilon_0}{2} \oint d^2 f_i n_L E_{iL} \Phi, \quad (4.23)$$

applying the Gauß identity to the first part of Green's identity (4.22). The second part of the identity (4.22) contains the Laplacian of Φ , which is vanishing. Due to our assumption that outside the lattice boundaries there is no charge density we have $\Delta \Phi = 0$.

⁵The soliton radius r_0 in multiples of lattice length a is one of the selectable parameters in the beginning of each simulation run.

Considering natural boundary conditions, the electrodynamic potential Φ of a dipole expressed in cylindrical coordinate space reads

$$\Phi = \frac{e_0}{4\pi\epsilon_0} \left(\frac{q^+}{\sqrt{r^2 + z_+^2}} + \frac{q^-}{\sqrt{r^2 + z_-^2}} \right), \quad (4.24)$$

where $z_+ = z + d$ and $z_- = z - d$. q^+ , q^- denote the charges of a dipole. Figure 4.1 illustrates the geometry of the dipole.

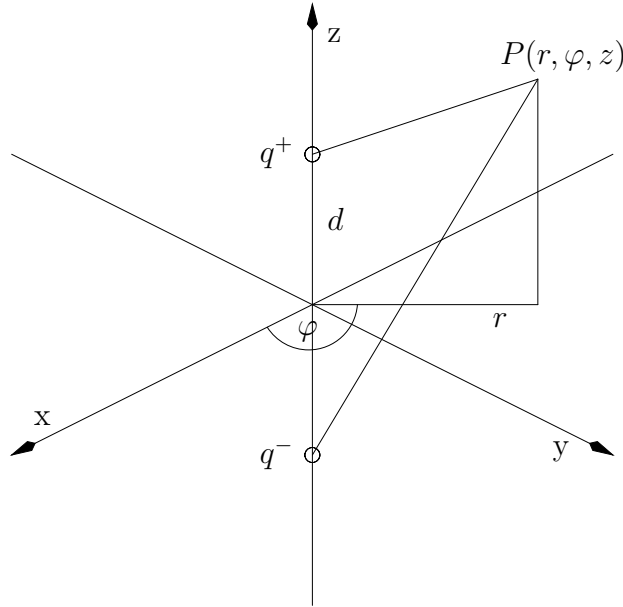


Figure 4.1: Arrangement of the two solitons of a dipole. q^+ , q^- indicate the positions $(0, 0, +d)$ and $(0, 0, -d)$, respectively.

4.2 Computation of action

We determine the soliton configuration by minimization of the total energy on the lattice. In the previous section 4.1 we have explicated how to calculate the total energy of a soliton configuration. This approach can be summarized as *gamma-action* [16, 17]. However, there is an alternative, computing the action on the lattice, it is denoted as *Wilson action* [19, 20].

In general, the action has to be invariant under gauge transformations, that means the physical laws do not change their explicit forms. Let us consider n complex scalar fields $\phi^i(x^\mu)$ with $i = 1, \dots, n$, which form the components of a complex vector field $\Phi(x^\mu)$. For each point x^ν the vector $\Phi(x^\mu)$ is an element of vector space \mathcal{V}_x , which is isomorphic to \mathbb{C}^n . The action S is defined by a

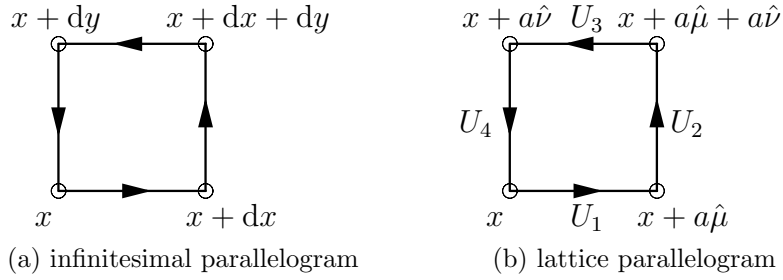


Figure 4.2: Infinitesimal parallelogram in the continuum and a plaquette on the lattice.

functional

$$S = \int d^4x \mathcal{L}(\Phi(x^\mu), \partial_\nu \Phi(x^\mu)) \quad (4.25)$$

with the Lagrange density $\mathcal{L} = \mathcal{L}(\Phi(x^\mu), \partial_\nu \Phi(x^\mu))$. S has to be invariant under a gauge transformation of the form

$$\Phi(x^\mu) \longrightarrow \Phi'(x^\mu) = \Lambda(x^\mu)\Phi(x^\mu) \quad \text{and} \quad \Lambda \in \mathbf{SU}(n), \quad (4.26)$$

whose properties have already been mentioned in table 2.1 in section 2.3.1. That means $\Lambda(x^\mu)$ is a $n \times n$ -matrix, which requires

$$\Lambda^\dagger \Lambda = \mathbb{1}_n, \quad \det[\Lambda] = 1.$$

Global gauge invariance is given if the gauge transformation of type (4.26) is independent of the coordinates⁶. Coordinate dependent $\Lambda = \Lambda(x^\mu)$ is labeled as *local* gauge transformation. Resulting from local-dependency of basis transformations, this requires a modification of the derivative and raises *parallel transport* and *covariant derivative*. As already addressed in section 2.5.3 for soliton field $Q(x^\mu)$, the concept of parallel transport is closely interrelated with the covariant derivative. An accurate derivation of this relation is given in appendix C.

4.2.1 Gauge fields and Wilson action

Evaluating the Wilson action on a lattice, the covariant derivative in continuous space (C.4) has to be amended by a version for a discrete grid. The soliton field $Q(x^\mu)$ possesses substantial values only at lattice points x^μ . A similar fact applies to the parallel transport U . Opposite to infinitesimal distances in continuum space dx^μ the shortest non-zero link between two neighbouring points is the lattice constant a . Thus, we introduce elementary parallel transporters $U_{x\mu}$ at x in $\hat{\mu}$ -direction with $\mu = 1, 2, 3, 4$ in case of an hypercubic

⁶In this case Λ is constant.

lattice⁷. The corresponding directed link b is a path from x to $x + a\hat{\mu}$ and is identified with ordered pairs of points on the lattice

$$b = \langle x + a\hat{\mu}, x \rangle \equiv (x, \mu) .$$

Assigning link b with the parallel transporter, that is denoted

$$U(b) \equiv U(x + a\hat{\mu}, x) \equiv U_{x\mu} \in \mathbb{G} , \quad (4.27)$$

where \mathbb{G} is the gauge group. The *Link variable* $U_{x\mu}$ satisfies reversibility

$$U(y, x) = U^{-1}(x, y) \quad (4.28)$$

and path composition

$$U(\mathcal{C}) = U(b_n) \dots U(b_1) = \prod_{b \in \mathcal{C}} U(b) \quad (4.29)$$

for an arbitrary path \mathcal{C} on the lattice

$$\mathcal{C} = b_n \circ \dots \circ b_2 \circ b_1 .$$

The set of all link variables $\{U(b)\}$ is considered as *lattice gauge field*. Under gauge transformations the link variables transform similarly to the continuum, Eq. (C.1), as

$$U'(y, x) = \Lambda^{-1}(y)U(y, x)\Lambda(x) . \quad (4.30)$$

In analogy to Eq. (C.2), we define the covariant derivative of the vector field C_ν by

$$D_\mu C_\nu = \frac{1}{a} (U^{-1}(x, \mu)C_\nu(x + a\hat{\mu}) - C_\nu(x)) . \quad (4.31)$$

Hence, by the previous definition we are able to replace ordinary derivatives in the kinetic part of the Lagrangian and to construct a gauge invariant expression

$$S = \frac{1}{2} \sum_x a^4 D_\mu C_\nu D_\mu C_\nu = -a^2 \sum_{x,y} C_\nu(x) U(x, y) C_\nu(y) + 4a^2 \sum_x C_\nu^2 \quad (4.32)$$

where

$$\sum_{x,y} C_\nu(x) U(x, y) C_\nu(y)$$

describes the nearest neighbour coupling.

Another gauge invariant quantity, regarding a closed curve $\mathcal{C}_{x,x}$, reads

$$S = \text{Tr} [U(\mathcal{C}_{x,x})] . \quad (4.33)$$

⁷As already mentioned at the beginning of this chapter 4, we have managed to examine the question on a two dimensional lattice, due to exploiting the symmetry.

This is used as starting point for the derivation of Wilson's action [20] in our model. Considering four neighbour points, see Fig. 4.2b, the smallest closed loops on the lattice are denominated *plaquettes*. Each tile consists of four links and we express a plaquette $p = (x; \mu\nu)$ by four vertices

$$x, \quad x + a\hat{\mu}, \quad x + a\hat{\mu} + a\hat{\nu}, \quad x + a\hat{\nu}.$$

The corresponding parallel transporter U_p is constructed as

$$U_p \equiv U_{x;\mu\nu} = U_4 U_3 U_2 U_1 \quad (4.34)$$

with

$$\begin{aligned} U_1 &= U(x + a\hat{\mu}, x), & U_2 &= U(x + a\hat{\mu} + a\hat{\nu}, x + a\hat{\mu}), \\ U_3 &= U(x + a\hat{\nu}, x + a\hat{\mu} + a\hat{\nu}), & U_4 &= U(x, x + a\hat{\nu}). \end{aligned}$$

U_p is called a *plaquette variable*. The action functional $S[U]$ of lattice gauge theory is the sum over all plaquette variables,

$$S[U] = \sum_p S_p(U_p) \quad (4.35)$$

with the following plaquette term for $\mathbf{SU}(n)$

$$\begin{aligned} S_p(U) &= -\beta \left[\frac{1}{2 \text{Tr}[\mathbb{1}_n]} (\text{Tr}[U] + \text{Tr}[U^{-1}]) - 1 \right] \\ &= \beta \left[1 - \frac{1}{n} \Re \text{Tr}[U] \right] \end{aligned} \quad (4.36)$$

and thereby β denotes the coupling constant. For each point x every plaquette term is included only with one orientation but with all directions

$$\sum_p \equiv \sum_x \sum_{\mu < \nu}.$$

Applying Wilson's action to the MTF on the lattice, we consider the soliton fields $Q(x)$ from Eq. (3.5) and the dual gauge field $C_\mu = -\frac{\alpha_f \hbar}{e_0} \Gamma_{\mu K} \frac{\sigma_K}{2}$, Eq. (3.1), with the generators $\sigma_K/2$. The affine connection $\Gamma_{\mu K}$ plays the role of the gauge field. Therefore, the parallel transporter $U(x, \mu)$ reads

$$\begin{aligned} U(x, \mu) &\equiv e^{iaC_\mu(x)} = e^{ia\beta\Gamma_{\mu K} \frac{\sigma_K}{2}} \\ &= 1 + ia\frac{\beta}{2}\Gamma_{\mu K}\sigma_K - a^2\frac{\beta^2}{8}\Gamma_{\mu K}\sigma_K\Gamma_{\mu L}\sigma_L - \dots \end{aligned} \quad (4.37)$$

with the prefactor $\beta = -\frac{\alpha_f \hbar}{e_0}$. Furthermore, discretising the definition of the derivative $\partial_\mu Q = i\Gamma_{\mu K}\sigma_K Q$ leads to a difference quotient. Rearranging

Eq. (2.79) yields

$$\begin{aligned} \frac{Q(x+a\hat{\mu})-Q(x)}{a} &= i\Gamma_{\mu K}\sigma_K Q \quad \Big| \cdot aQ^\dagger(x) \\ Q(x+a\hat{\mu})Q^\dagger(x) &= 1 + ia\Gamma_{\mu K}\sigma_K \\ &\approx e^{ia\Gamma_{\mu K}\sigma_K}. \end{aligned} \quad (4.38)$$

Comparing Eq. (4.37) with Eq. (4.38), we obtain for the parallel transporter $U_\mu(x)$

$$U_\mu(x) = \sqrt{Q(x+a\hat{\mu})Q^\dagger(x)} \approx e^{ia\Gamma_{\mu K}\frac{\sigma_K}{2}}. \quad (4.39)$$

Hence, inserting Eq. (4.39) in Eq. (4.34), the plaquette variable U_p can be calculated

$$U_p = e^{ia^2\varepsilon_{KLM}\Gamma_{\mu K}\Gamma_{\nu L}\frac{\sigma_M}{2}} = e^{ia^2R_{\mu\nu M}\frac{\sigma_M}{2}}. \quad (4.40)$$

To gather the full expression of Wilson's action on the lattice, the above interim result has to be applied to Eq. (4.36). Therefore, we use⁸

$$\frac{1}{2}(\text{Tr}[U] + \text{Tr}[U^{-1}]) = 1 - \frac{1}{8}a^4 \text{Tr}[R_{\mu\nu K}\sigma_K R_{\mu\nu L}\sigma_L]$$

that is

$$\begin{aligned} S_p(U) &= -\beta \left[\frac{1}{\text{Tr}[\mathbb{1}_2]} \left(1 - \frac{1}{8}a^4 \text{Tr}[R_{\mu\nu K}\sigma_K R_{\mu\nu L}\sigma_L] \right) - 1 \right] \\ &= -\beta \left[-\frac{1}{2} - \frac{1}{16}a^4 \text{Tr}[R_{\mu\nu K}R_{\mu\nu L}\delta_{KL}] \right] \\ &= \frac{\beta}{8}a^4 (R_{\mu\nu K})^2, \end{aligned} \quad (4.41)$$

where the constant 1/2 is neglected and the identity $\text{Tr}[R_{\mu\nu K}R_{\mu\nu L}\delta_{KL}] = 2(R_{\mu\nu K})^2$ was used. Summing over all plaquettes taking into account single counting of p , we obtain the action functional of Eq. (4.35)

$$S[U] = \sum_p S_p = \frac{\beta}{8}a^4 \sum_p (R_{\mu\nu K})^2 = \frac{\beta}{16}a^4 \sum_{\mu,\nu} (R_{\mu\nu K})^2. \quad (4.42)$$

⁸Evaluating Taylor expansion of Eq. (4.40), that is

$$\begin{aligned} U_p &= 1 + ia^2 R_{\mu\nu K} \frac{\sigma_K}{2} - \frac{1}{2}a^4 R_{\mu\nu K} \frac{\sigma_K}{2} R_{\mu\nu L} \frac{\sigma_L}{2} + \mathcal{O}(a^6), \\ U_p^\dagger &= 1 - ia^2 R_{\mu\nu K} \frac{\sigma_K}{2} - \frac{1}{2}a^4 R_{\mu\nu K} \frac{\sigma_K}{2} R_{\mu\nu L} \frac{\sigma_L}{2} + \mathcal{O}(a^6). \end{aligned}$$

Disregarding terms of higher order than a^4 , the sum is

$$U_p + U_p^\dagger = 2 - \frac{1}{4}a^4 R_{\mu\nu K} R_{\mu\nu L} \delta_{KL}.$$

Chapter 5

Results

5.1 Using Computer program `sol`

The computer procedures, written by Joachim Wabnig [16], have been re-designed in regard to acceleration of execution. However, the main concept and workflow diagrams have been kept unmodified, despite of some supplements in the formula for the total energy. In the lattice simulation we have examined configurations of two solitons. As already mentioned in chapter 3.4, a cylindrical grid model has been initialized. In this geometry all further calculations have been performed. The lattice simulation program, `sol`, has been formulated in the computer language "C". This program, presuming the appropriate directory, is manually executed by command line:

```
$ ./sol [options] [filename] ↵
```

Table 5.1: The parameter `[filename]` in this command line indicates the start configuration of the soliton field. Table D.1 contains a detailed description of the available `[options]`.

The general program flow of `sol` is sketched in Fig. 5.1. At the beginning, but after some less important initialisation of variables, the program evaluates the parameters passed on the command line. Those parameters control the main routine and are responsible of branching into different subprocedures. All parameters passed, described in more detail in compound table D.1 in appendix D, are optional. If any parameters are skipped, a default behaviour will be assumed by calculating a default soliton configuration, defined in the source code file `definition.h`.

The initially computed soliton configuration is stored as an array of pairs of numbers for the soliton field components $q_r(r, z)$ and $q_z(r, z)$. As already detailed in the previous Sec. 4, the total energy obtained on the lattice is calculated and the loop is entered. Running the loop implies the periodic call of the subprocedure `powell.c`, copied from the book Numerical Recipes [18].

Initialisation of startvalues		
Evaluation of passed options and parameter		
Branch to different procedures		
Load and caculate an existing configuration	initialize lattice monopole configuration	initialize lattice dipole configuration
Compute energy of curvature E_c potential energy E_{pot} residual energy E_{out}	Compute energy of curvature E_c potential energy E_{pot} residual energy E_{out}	Compute energy of curvature E_c potential energy E_{pot} residual energy E_{out}
	loop: minimize total energy of soliton	loop: minimize total energy of solitons
output results to screen and save to file		
gnuplot soliton		

Figure 5.1: A simplified flowchart of computer program `sol`, calculating total energy of solitons on a lattice simulation.

It is responsible for minimizing the total energy of the soliton configuration by varying the components of the soliton field $Q(x)$. The exit condition depends on a comparison of the total energies of two consecutive energy minimizing procedure calls without noteworthy difference. The cut-of-value is specified in the file `definition.h`. Due to this termination condition we assume the resulting soliton field is in a locally minimized and stable configuration.

For small distances the attraction between the partners of a soliton pair, the minimization procedure `powell.c` reflects the instability of such a configuration. This instability has been suppressed by fixing the field within the radius \bar{r}_0 of each of the two solitons. Consequently, Powell's procedure modifies the soliton field only beyond a distance of one soliton radius. Therefore Powell's routine has not always caught the global energy minima.

In the majority of more than five hundred iterations the soliton field configurations have been completely deranged. Therefore, a maximum number of loop-iterations has been chosen as a second exit condition and consequently

the computed results have been discarded. Final and reasonable outputs are stored automatically in text-files with a default filename. The latter can be used conveniently by gnuplot, demonstrating a decorative plot.

5.2 Accuracy

For a first test of the accuracy of the numerical calculations, we have used a one-soliton configuration with different radii and lattices with different sizes. We have computed the total energy $H_{\text{tot}} = \sum H_x$ of a lattice configuration and consequently the radius of the single soliton, located at the origin. Recapitulating section 3.2.1, we already know the algebraic solution of a soliton monopole. Thereby we have assumed a parameter $m = 3$ of the soliton potential's energy density $\Lambda(q_0) = q_0^{2m}/r_0$. In Tab. 5.2, we specify the computed total energy $\sum H_x$ for a given lattice size ($N_Z \times N_R$) and an assumed soliton radius \bar{r}_0 in units of the lattice spacing a . Using Eq. (3.29), we are able to derive the soliton radius r_0 in fm. The computed total energy is composed of the curvature energy H_c and the potential energy H_{pot} – both values are calculated on the lattice. In addition, the energy contribution H_{out} of the remaining space, outside the considered lattice-volume, is calculated by a numerical determination of the integral (4.15).

We compare these numerical results with the algebraic one-soliton solution of Sec. 3.2.1, Eq. (3.29). This is illustrated in table 5.2. The algebraic value $r_0 = 2.21$ fm and the numerical value differ by less than one percent only. The last column refers to the integrals in Eq. (3.28) describing the energy of the radial electric field, the tangential electric field and the potential energy of the one-soliton configuration. These integrals predict for the energy ratio $(H_c + H_{\text{pot}})/H_{\text{pot}}$ a value of 4. Therefore, the last column gives an indication of the accuracy of the numerical calculations. The deviation of the last column from the predicted value, indicates the influence of lattice artifacts. Obviously, the bigger the lattice size, the smaller the deviations and the higher is the accuracy of the results. This fact is simply traced back to numerical spikes, raised mainly in numerical derivatives on the lattice. Hence, the bigger the lattice size for the computed values of the soliton field $Q(x)$ the better – the lattice becomes smoother.

In the upper third of table 5.2 the data set for the lattice size 41×20 shows first an increase of the accuracy by about half a percent, but with growing soliton radius, at $N_R, N_Z \approx 3\bar{r}_0$ the ratio starts to deteriorate. We conclude, that we have to pay attention to the ratio of lattice size and soliton radius.

\bar{r}_0	a	r_0	H_c	H_{pot}	H_{out}	$\sum H_x$	$\frac{H_c+H_{\text{pot}}}{H_{\text{pot}}}$
Lattice size $(N_Z \times N_R)$ 41×20							
2	1.0900 fm	2.180 fm	0.2674	0.0963	0.0230	0.3868	4.02
3	0.7317 fm	2.195 fm	0.1726	0.0644	0.0227	0.2596	4.03
4	0.5485 fm	2.194 fm	0.1243	0.0482	0.0222	0.1946	4.04
5	0.4365 fm	2.183 fm	0.0951	0.0383	0.0215	0.1549	4.05
6	0.3605 fm	2.163 fm	0.0756	0.0315	0.0208	0.1279	4.06
8	0.2626 fm	2.101 fm	0.0512	0.0228	0.0192	0.0932	4.09
10	0.2011 fm	2.011 fm	0.0368	0.0173	0.0173	0.0714	4.13
Lattice size $(N_Z \times N_R)$ 91×35							
2	1.0895 fm	2.179 fm	0.2778	0.0965	0.0123	0.3866	4.01
3	0.7324 fm	2.197 fm	0.1830	0.0646	0.0123	0.2599	4.02
4	0.5508 fm	2.203 fm	0.1346	0.0486	0.0122	0.1955	4.02
5	0.4409 fm	2.205 fm	0.1054	0.0390	0.0121	0.1565	4.02
6	0.3671 fm	2.203 fm	0.0859	0.0324	0.0120	0.1303	4.02
8	0.2741 fm	2.192 fm	0.0614	0.0242	0.0117	0.0973	4.02
10	0.2174 fm	2.174 fm	0.0467	0.0192	0.0113	0.0771	4.03
Lattice size $(N_Z \times N_R)$ 101×40							
2	1.0894 fm	2.179 fm	0.2793	0.0965	0.0108	0.3866	4.01
3	0.7324 fm	2.197 fm	0.1845	0.0647	0.0108	0.2599	4.02
4	0.5510 fm	2.204 fm	0.1361	0.0487	0.0107	0.1955	4.02
5	0.4412 fm	2.206 fm	0.1069	0.0390	0.0107	0.1565	4.01
6	0.3675 fm	2.205 fm	0.0874	0.0325	0.0106	0.1304	4.01
8	0.2749 fm	2.199 fm	0.0629	0.0243	0.0104	0.0975	4.01
10	0.2186 fm	2.186 fm	0.0482	0.0193	0.0101	0.0776	4.02

Table 5.2: This table compares the numerical values with the algebraic solution for a one-soliton configuration. The columns denote from left to right: soliton radius \bar{r}_0 in lattice units a , lattice constant a in fm, soliton radius $r_0 = a\bar{r}_0$ in fm, total curvature energy H_c , total potential energy H_{pot} , electrostatic energy H_{out} outside the lattice volume, sum of all energy contributions $\sum H_x = H_c + H_{\text{pot}} + H_{\text{out}}$ and energy ratio $(H_c+H_{\text{pot}})/H_{\text{pot}}$. All these energies are in units of $\frac{\alpha_f \hbar c}{a}$.

5.2.1 Boundary conditions

As already stated in Sec. 3.1, the shape of the hedgehog field far away from the soliton centers ensures to approach in the electrodynamic limit Coulomb's r^{-2} -law. The soliton field is moving towards the equator of \mathcal{S}^3 and the q_0 -component is vanishing. In the one-soliton configuration with Eq. (3.27) we obtain for q_0

$$q_0 = \cos \alpha(\rho) = \frac{r_0}{\sqrt{r_0^2 + r^2}}. \quad (5.1)$$

$N_Z \times N_R$	d	\bar{r}_0	H_{out}	$R_{\text{fixed}} = 4a$		$R_{\text{fixed}} = 2a$
				$H_c + H_{\text{pot}}$	H_{tot}	H_{tot}
130×65	8	3.0	$5.5 \cdot 10^{-5}$	0.3741	0.3742	
130×65	10	3.0	$8.6 \cdot 10^{-5}$	0.4044	0.4045	
73×30	12	3.0	0.0010	0.4251	0.4262	0.4158
75×30	14	3.0	0.0014	0.4400	0.4414	0.4335
79×30	18	3.0	0.0022	0.4588	0.4609	0.4521
85×30	24	3.0	0.0035	0.4735	0.4770	0.4697
91×30	30	3.0	0.0050	0.4811	0.4861	0.4792
97×30	36	3.0	0.0065	0.4856	0.4921	0.4853
103×30	42	3.0	0.0080	0.4882	0.4963	0.4895
109×30	48	3.0	0.0095	0.4899	0.4994	0.4926
115×30	54	3.0	0.0108	0.4909	0.5018	0.4951
121×30	60	3.0	0.0121	0.4916	0.5037	0.4970
127×30	66	3.0	0.0132	0.4920	0.5053	0.4985
133×30	72	3.0	0.0143	0.4923	0.5066	0.4998
139×30	78	3.0	0.0152	0.4924	0.5077	0.5009
151×30	90	3.0	0.0168	0.4926	0.5094	0.5027
166×30	105	3.0	0.0185	0.4926	0.5111	0.5043

Table 5.3: The total energy for different lattice sizes and different soliton distances. The first three columns indicate the lattice size $N_Z \times N_R$, the distance d of soliton centers and the soliton radii \bar{r}_0 in lattice units a . The next three columns display the cross border energy H_{out} , the sum of the curvature energy H_c and the potential energy H_{pot} the total energy $H_{\text{tot}} = \sum H_x$. The last column shows the total energy H_{tot} , but with different R_{fixed} . All energies are denoted in units of $\alpha_f \hbar c/a$.

Let us consider an upper bound $q_0 = 10^{-1}$, below this bound the potential energy, which is of order $\mathcal{O}(q_0^{2m})$, becomes insignificant. From Eq. (5.1) we conclude that we reach this bound at $r = 10 r_0$.

We always start from a soliton configuration, which is close to the minimum. For the dipole configuration we locate the two solitons at the given distance d symmetrically in the positive and negative z -region. At $z = 0$ this start configuration suffers from discontinuities. However, Powell's minimization process smooths these discontinuities.

With decreasing distance between the soliton centers the numerical difficulties increase due to instabilities of the soliton field. To circumvent this problem, it is necessary to fix the soliton fields around the soliton centers. The corresponding region has been widened until the lattice calculations got stable minima.

5.3 Dipole results

As already stated, we investigate soliton-soliton collisions by computing snapshots for different distances of the soliton centers. According to the above mentioned bound $q_0 = 10^{-1}$ we have to choose an appropriately large lattice. E.g. for $r_0 = 3a$, we have to provide at least distances of $30a$ in each direction from the soliton centers. Referring to [16], for decreasing distances of the soliton centers we anticipate increasing deviations from Coulomb's law.

In Tab. 5.3 the computed values of the total energy are displayed for different distances of the soliton centers. The first three columns show the starting parameter, the lattice size $N_Z \times N_R$, the distance d of soliton centers and the soliton radii \bar{r}_0 in lattice units a . The next two columns are energy contributions, the total cross border energy H_{out} and the sum of the curvature energy H_c and the potential energy H_{pot} . The last two columns display the results for the sum H_{tot} of the energy contributions for different values of R_{fixed}

$$H_{\text{tot}} = H_c + H_{\text{pot}} + H_{\text{out}} = \sum H_x. \quad (5.2)$$

The energy values are again denoted in units of $\alpha_f \hbar c/a$. The smaller the

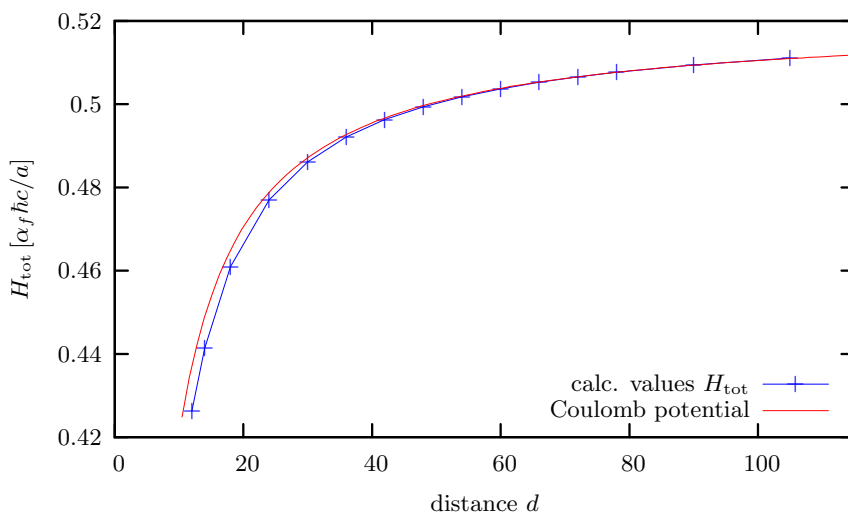


Figure 5.2: H_{tot} according to Tab. 5.3 with a fixed radius $R_{\text{fixed}} = 4a$ as a function of the soliton distance $d = r/a$ in lattice units. This is compared to twice the rest energy $m_e c^2$ and the $1/r$ -potential of the Coulomb interaction. For small soliton distances the energy values deviate from the Coulomb potential.

distance $r = da$ of the soliton cores, the stronger is the attraction between the solitons and the more caution is necessary to inhibit a collapse of the numerical

minimisation. As soon as there is a sign for such a collapse the program is restarted with larger regions with fixed soliton field¹.

In Fig. 5.2 the numerical results for H_{tot} are plotted. The energy curve shows two times the rest mass of an electron $2m_e c^2$ minus the electromagnetic interaction energy. For point-like charges the interaction energy is described by the usual $1/r$ -potential with $r = da$

$$H_{\text{point}} = 2m_e c^2 - \frac{\alpha_f \hbar c}{r}, \quad \alpha_f = \frac{e_0^2}{4\pi\epsilon_0 \hbar c}, \quad (5.3)$$

also drawn in Fig. 5.2 for comparison. The deviations of H_{tot} from the point-like behaviour at small distances d can be interpreted as a variation of the soliton charge $e_0 Q(d)$ or the fine structure constant $\alpha_f Q^2(d)$ leading to

$$H_{\text{tot}}(d) = 2m_e c^2 - Q^2(d) \frac{\alpha_f \hbar c}{r} \quad \text{for } r = da. \quad (5.4)$$

It is interesting to look more carefully at the behaviour of the “effective”

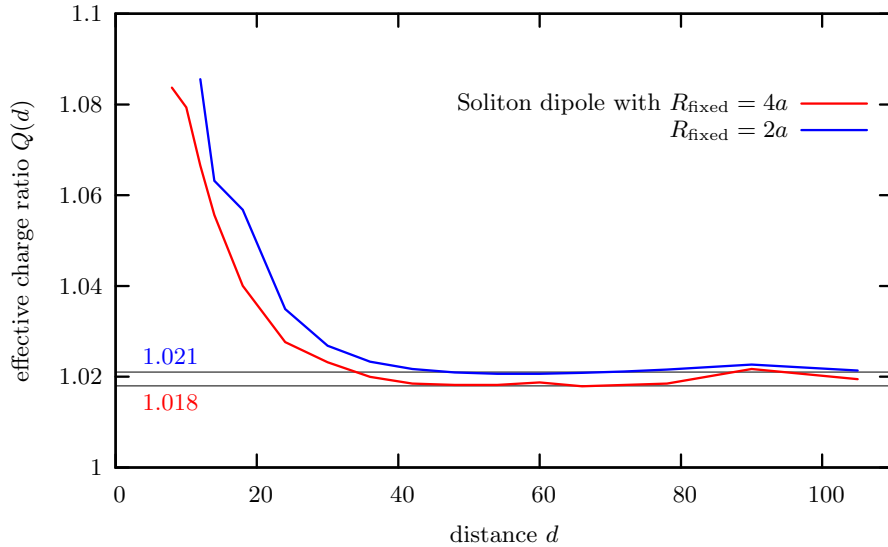


Figure 5.3: From the energy values in Tab. 5.3 we determine the effective charge ratios $Q(d)$ according to Eq. (5.4). For small distances we observe a strong increase of $Q(d)$. Concerning the asymptotic value for large d we observe a dependence on R_{fixed} since with decreasing R_{fixed} the minimization has to be stopped earlier leading to asymptotic charges greater than 1.

charge $Q(d)$ in Eq. (5.4). Its values are plotted in Fig. 5.3 for two values of

¹For soliton core distances $d \geq 12a$, it is possible to use a fixation radius of $2a$. Below this distance a radius $R_{\text{fixed}} = 3a$ or larger is used.

R_{fixed} . In the asymptotic region $d > 40a$ the effective charge ratio approaches a constant, but the value of this constant depends on the value of R_{fixed} . This can be explained by the numerical inaccuracy in the determination of the rest mass of single solitons and their deviation from the analytic result $\frac{\alpha_f \hbar c}{a} \frac{\pi}{4}$.² This deviation is due to the contribution of the cross-border energy H_{out} to H_{tot} differing from the corresponding analytic contribution. To compensate for this error we introduce a parameter μ depending on R_{fixed} shifting the rest mass of the two solitons and get by this modification of Eq. (5.4) the effective charge ratio

$$Q(d) = \sqrt{\frac{2m_e c^2 - \mu - H_{\text{tot}}(d)}{\alpha_f \hbar c}} r \quad \text{for } r = da. \quad (5.5)$$

Fig.5.3 shows that for distances $d < 40a$ the effective charge ratio gets an additional contribution. In the region $d > 10a$ this contribution can be approximated by a *exponentially* decreasing function. This is a behaviour analogous to the Sine-Gordon model, where in a kink-kink collision the kinks contract and the energy stored in the kinks increases. In the moment of closest approach the profile function $\phi(x, t)$ gets the highest values of the derivative $\frac{\partial \phi}{\partial x}$ [16].

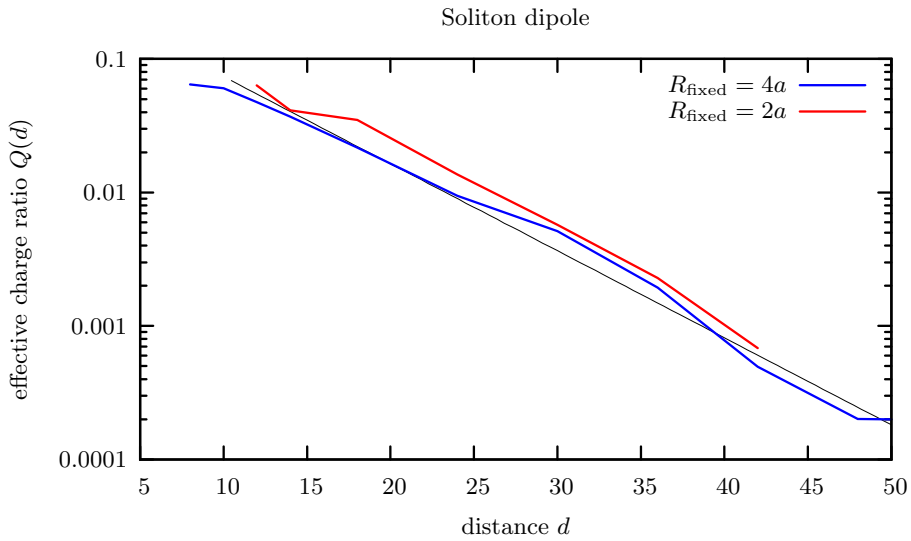


Figure 5.4: A closer look at Fig. 5.3 at tight soliton distances reveals the exponential behaviour of the effective charge ratio $Q(d)$. The black line is a fitted exponential function.

²See Sec. 3.2.1, p. 30.

$N_Z \times N_R$	d	\bar{r}_0	$R_{\text{fixed}} = 4a$			$R_{\text{fixed}} = 2a$		
			H_{tot}	H_c	S_{wilson}	H_{tot}	H_c	S_{wilson}
166 × 30	105	3.0	0.5111	0.3599	0.3284	0.5101	0.3629	0.3563
151 × 30	90	3.0	0.5094	0.3598	0.3283	0.5084	0.3628	0.3564
139 × 30	78	3.0	0.5077	0.3595	0.3283	0.5066	0.3626	0.3565
133 × 30	72	3.0	0.5066	0.3593	0.3282	0.5055	0.3624	0.3565
127 × 30	66	3.0	0.5053	0.3589	0.3281	0.5042	0.3621	0.3566
121 × 30	60	3.0	0.5037	0.3584	0.3280	0.5026	0.3616	0.3567
115 × 30	54	3.0	0.5018	0.3575	0.3279	0.5007	0.3609	0.3568
109 × 30	48	3.0	0.4994	0.3562	0.3276	0.4983	0.3597	0.3569
103 × 30	42	3.0	0.4963	0.3542	0.3272	0.4951	0.3579	0.3571
97 × 30	36	3.0	0.4921	0.3510	0.3266	0.4909	0.3549	0.3573
91 × 30	30	3.0	0.4861	0.3457	0.3254	0.4849	0.3501	0.3577
85 × 30	24	3.0	0.4770	0.3363	0.3231	0.4754	0.3413	0.3586
79 × 30	18	3.0	0.4609	0.3181	0.3170	0.4580	0.3227	0.3624
			$R_{\text{fixed}} = 4a$			$R_{\text{fixed}} = 3a$		
75 × 30	14	3.0	0.4414	0.2944	0.3060	0.4392	0.2941	0.3208
73 × 30	12	3.0	0.4262	0.2759	0.2946	0.4218	0.2730	0.3189
130 × 65	10	3.0	0.4045	0.2508	0.2754			
130 × 65	8	3.0	0.3742	0.2158	0.2443			

Table 5.4: Data for soliton dipoles with the same parameters as in Tab. 5.3: Soliton distance d , radii \bar{r}_0 are in lattice units a , the total energy H_{tot} and the curvature energy H_c in units of $\alpha_f \hbar c/a$. The values of the Wilson action, Eq. (5.6) for $\beta = 1$ are added in the columns, entitled S_{wilson} .

In the region $5 < d < 50$ the effective charge ratio $Q(d)$ can be approximated by an exponential function, as shown in Fig. 5.4.

Wilson action

For verification purposes, we calculate the average plaquette action with the Wilson action for different lattice sizes. According to Eq. (4.35) and Eq. (4.42) we get

$$S[U] = \sum_p S_p = \frac{\beta}{8} a^4 \sum_p (R_{\mu\nu K})^2 = \frac{\beta}{16} a^4 \sum_{\mu,\nu} (R_{\mu\nu K})^2. \quad (5.6)$$

The results of $S[U]$ for $\beta = 1$ are shown in Tab. 5.4 and plotted in Fig. 5.5. The first three columns in Tab. 5.4 show the lattice size $N_Z \times N_R$, the distance d and the soliton radii \bar{r}_0 in lattice units a . Columns 4 and 5 give the values of the total energy H_{tot} and the curvature energy H_c in units of $\alpha_f \hbar c/a$ and the Wilson action $S[U]$ for $R_{\text{fixed}} = 4a$. Columns 7 to 9 show the same items

for $R_{\text{fixed}} = 2a$. Unfortunately the lattice calculations collapse for extra small distances and less fixation due to the strong interaction leading to annihilation.

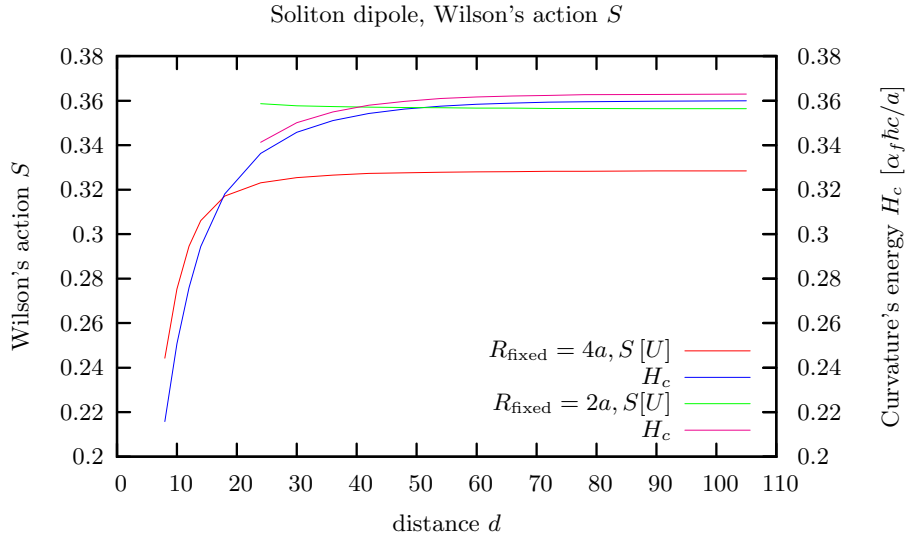


Figure 5.5: Wilson action S of Eq. (5.6) for $\beta = 1$ and curvature energy H_c in units of $\frac{\alpha_f \hbar c}{a}$ for the dipole configuration. In a good approximation both functions approach exponentially a constant value. For $R_{\text{fix}} = 2a$ the lattice calculations did not converge for small distance d between the charges.

Resulting data from Tab. 5.4 are plotted in Fig. 5.5 for better comparison between the curvature energies and the Wilson action. Both graphs of H_c and $S[U]$ show the same characteristic. For small distances d of the solitons the action gets a contribution decreasing exponentially with d , like the curvature energy. Due to different units, the numbers in the columns of H_c and S in Tab. 5.4 can not be compared directly. Similarly, different values of R_{fixed} and hence different minimization regions lead to different numerical values of the Wilson action.

5.4 Conclusion

The *model of topological fermions* (MTF) is based on a $\mathbf{SU}(2)$ scalar field theory with a Lagrangian allowing stable solitonic solutions with long range Coulombic interaction. In this model the electrodynamic properties of particles can be deduced. Far away from soliton centres, denoted the *electrodynamic limit*, solitons appear as point-like charges and behave as expected from Maxwell's theory. Due to the topological constraints and without the

necessity of quantizing the MTF itself, the MTF already describes quantized charges and even spin. However, unlike the common picture, the MTF considers charged particles of finite size and avoids singularities.

We have shown by choosing this special field theory that the curvature tensor $R_{\mu\nu KM}$ derived from the $\mathbf{SU}(2)$ field coincides with the dual electric field tensor $*F_{\mu\nu KM}$ up to a constant dimensional factor. This assumption allows to calculate the soliton field $Q(x^\mu)$ from a known potential. Consequently, we derive the equation of motion for the soliton field according to the principles of field theory. Due to the difficulty of solving the resulting differential equation for two colliding solitons, we have developed a lattice computer simulation. It allows to calculate static snapshots at narrowing distances of both particles. The numerical results are presented in tables and figures.

The energy of a dipole system can be separated in the rest-mass of non-interacting solitons and the interaction energy, behaving at large distances as expected for charged particles. With decreasing size of the dipole the charge values of the solitons start to deviate from the unit charge. The effective charge gets at small distances a contribution decaying exponentially with the separation of the dipole. An effect which can be denoted as *running coupling*.

Appendix A

Equation of motion

A variation of soliton field $Q(x^\mu) = q_0(x^\mu) + i\sigma_K q_K(x^\mu)$ has to respect the condition $q_0^2 + q_K q_K = 1$. Therefore, we multiply Q with an element of $\mathbf{SU}(2)$, $e^{i\sigma_K \zeta_K}$, close to the unit matrix, i.e. small values ζ_K

$$Q \longrightarrow Q' = e^{i\sigma_K \zeta_K} Q \quad (\text{A.1})$$

Expanding the exponential function to first order in ζ_K and using the identity $\sigma_K \sigma_L = \delta_{KL} + i\varepsilon_{KLM} \sigma_M$ we get

$$\begin{aligned} Q' &= e^{i\sigma_K \zeta_K} Q = \left[1 + i\sigma_K \zeta_K + \mathcal{O}(i\sigma_K \zeta_K)^2 \right] (q_0 + i\sigma_L q_L) \\ &= q_0 - \zeta_K q_K + i\sigma_K (q_K + q_0 \zeta_K + \varepsilon_{KLM} q_L \zeta_M) \end{aligned} \quad (\text{A.2})$$

So the virtual displacements become

$$\begin{aligned} \delta q_0 &= -\zeta_K q_K \\ \delta q_K &= q_0 \zeta_K + \varepsilon_{KLM} q_L \zeta_M \\ \delta Q &= Q(x^\mu + \delta x^\mu) - Q(x^\mu) \\ &= [q_0 + \delta q_0 + i\sigma_K (q_K + \delta q_K)] - [q_0 + i\sigma_K q_K] \\ &= i\sigma_K \zeta_K Q \\ \delta Q^\dagger &= -iQ^\dagger (\zeta_K \sigma_K). \end{aligned} \quad (\text{A.3})$$

This leads to

$$\begin{aligned} \partial_\mu \delta Q &= i [\partial_\mu \zeta_K \sigma_K Q + \zeta_K \sigma_K \partial_\mu Q] \\ &= [i\partial_\mu \zeta_K \sigma_K - \zeta_K \sigma_K \Gamma_{\mu L} \sigma_L] Q \end{aligned} \quad (\text{A.4})$$

and using Eq. (2.81) to

$$\begin{aligned} \delta \Gamma_{\mu K} &= \frac{1}{2i} \text{Tr} \left[\partial_\mu (Q + \delta Q) (Q^\dagger + \delta Q^\dagger) \sigma_M - \partial_\mu Q Q^\dagger \sigma_M \right] \\ &= \frac{1}{2i} \text{Tr} \left[\partial_\mu Q \delta Q^\dagger \sigma_M + \partial_\mu \delta Q Q^\dagger \sigma_M \right] \\ &= \frac{1}{2i} \text{Tr} \left[\Gamma_{\mu K} \sigma_K \zeta_L \sigma_L \sigma_M + i\partial_\mu \zeta_K \sigma_K \sigma_M - \zeta_K \sigma_K \Gamma_{\mu L} \sigma_L \sigma_M \right] \\ &= \partial_\mu \zeta_K + \text{Tr} \left[\Gamma_{\mu K} \zeta_L \varepsilon_{KLN} \sigma_N \sigma_M \right] = \partial_\mu \zeta_K + 2\varepsilon_{KLN} \Gamma_{\mu L} \zeta_M. \end{aligned} \quad (\text{A.5})$$

With Eq. (A.5) the variation $\delta R_{\mu\nu K}$ of the curvature tensor (2.98) $R_{\mu\nu K} = \varepsilon_{KLM}\Gamma_{\mu L}\Gamma_{\nu M}$ reads

$$\begin{aligned}\delta R_{\mu\nu K} &= \varepsilon_{KLM}\delta\Gamma_{\mu L}\Gamma_{\nu M} + \varepsilon_{KLM}\Gamma_{\mu L}\delta\Gamma_{\nu M} \\ &= \varepsilon_{KLM}[(\partial_\mu\zeta_L + 2\varepsilon_{LNP}\Gamma_{\mu N}\zeta_P)\Gamma_{\nu M} + \Gamma_{\mu L}(\partial_\nu\zeta_M + 2\varepsilon_{MNP}\Gamma_{\nu N}\zeta_P)] \\ &= \varepsilon_{KLM}(\partial_\mu\zeta_L\Gamma_{\nu M} - \partial_\nu\zeta_L\Gamma_{\mu M}) - 2(\Gamma_{\mu K}\Gamma_{\nu L}\zeta_L - \Gamma_{\nu K}\Gamma_{\mu L}\zeta_L)\end{aligned}\quad (\text{A.6})$$

Due to $\Gamma_{\mu K}R_K^{\mu\nu} = 0$ we find a scalar triple product by varying the squared curvature

$$\delta(R_{\mu\nu K}R_K^{\mu\nu}) = 2\delta R_{\mu\nu K}R_K^{\mu\nu} = 4\varepsilon_{KLM}\partial_\mu\zeta_L\Gamma_{\nu M}R_K^{\mu\nu}\quad (\text{A.7})$$

This result we insert in the variation of lagrangian density (3.22)

$$\begin{aligned}-\frac{4\pi}{\alpha_f\hbar c}\delta\mathcal{L} &= \delta\left(\frac{1}{4}R_{\mu\nu K}R_K^{\mu\nu} + \Lambda(q_0)\right) \\ &= \varepsilon_{KLM}\partial_\mu\zeta_L\Gamma_{\nu M}R_K^{\mu\nu} - \zeta_K q_K \partial_{q_0}\Lambda\end{aligned}\quad (\text{A.8})$$

Since ζ_K is the variation of generalised coordinates, $\partial_\mu\zeta_K$ are generalised velocities. Using Eq. (A.8) we derive the generalised momenta

$$\pi^\mu = \frac{\partial\mathcal{L}}{\partial\partial_\mu\zeta_K} = -\frac{\alpha_f\hbar c}{4\pi}\varepsilon_{KLM}\Gamma_{\nu L}R_M^{\mu\nu}\quad (\text{A.9})$$

Considering *Hamilton's principle* the action has to be minimal and therefore the variation of action has to vanish, $\delta S = 0$. After integration by parts, we get

$$\begin{aligned}0 &= \frac{4\pi}{\alpha_f\hbar c}\delta S = \frac{4\pi}{\alpha_f\hbar c}\int d^4x\delta\mathcal{L} \\ &= \int d^4x\zeta_K[q_K\partial_{q_0}\Lambda + \partial_\mu(\varepsilon_{KLM}\Gamma_{\nu L}R_M^{\mu\nu})]\end{aligned}\quad (\text{A.10})$$

Since the variation ζ_K is arbitrary we get the equation of motion

$$q_K\frac{d\Lambda}{dq_0} + \partial_\mu(\varepsilon_{KLM}\Gamma_{\nu L}R_M^{\mu\nu}) = 0.\quad (\text{A.11})$$

This is a generalisation of *Newton's second axiom* [23] and describes the interaction between solitons and electromagnetic fields.

Appendix B

Electric field of a dipole

We consider a dipole in the *electrodynamic limit* $q_K = n_K$ and determine the components of the electric field $\vec{E} = (E_1, E_2, E_3)^T = (E_\rho, E_\varphi, E_z)^T$. The soliton centers are located on the 3-axis with the negative charge $-e_0$ at $z = a$ and the positive charge e_0 at position $z = -a$, respectively. Using cylindrical coordinates and due to cylindrical symmetry, there is no field-strength in φ -direction. Hence, the differential equation is

$$\frac{d\rho}{E_\rho} = \frac{dz}{E_z} \quad (\text{B.1})$$

with the field components (3.40)

$$\begin{aligned} E_\rho(\rho, z) &= \frac{e_0}{4\pi\epsilon_0} \left[\frac{\rho}{r_+^3} - \frac{\rho}{r_-^3} \right] \\ E_z(\rho, z) &= \frac{e_0}{4\pi\epsilon_0} \left[\frac{z_+}{r_+^3} - \frac{z_-}{r_-^3} \right]. \end{aligned} \quad (\text{B.2})$$

With the abbreviations

$$z_\pm = z \pm a, \quad u = \frac{z_+}{\rho}, \quad v = \frac{z_-}{\rho} \quad (\text{B.3})$$

$$r_\pm = \sqrt{\rho^2 + z_\pm^2}, \quad r_+ = \rho\sqrt{u^2 + 1}, \quad r_- = \rho\sqrt{v^2 + 1} \quad (\text{B.4})$$

the electric field (B.2) becomes

$$\begin{aligned} E_\rho(\rho, z) &= \frac{e_0}{4\pi\epsilon_0} \frac{1}{\rho^2} \left[\frac{1}{\sqrt{(u^2 + 1)^3}} - \frac{1}{\sqrt{(v^2 + 1)^3}} \right] \\ E_z(\rho, z) &= \frac{e_0}{4\pi\epsilon_0} \frac{1}{\rho^2} \left[\frac{u}{\sqrt{(u^2 + 1)^3}} - \frac{v}{\sqrt{(v^2 + 1)^3}} \right]. \end{aligned} \quad (\text{B.5})$$

and the differential Eq. (B.1) is

$$\frac{d\rho}{\sqrt{(v^2 + 1)^3} - \sqrt{(u^2 + 1)^3}} = \frac{dz}{u\sqrt{(v^2 + 1)^3} - v\sqrt{(u^2 + 1)^3}}. \quad (\text{B.6})$$

Rewriting the shortcuts (B.3)

$$\rho(u+v) = 2z, \quad \rho(u-v) = 2a \quad \text{and} \quad \rho = \frac{2a}{u-v}, \quad z = a \frac{u+v}{u-v} \quad (\text{B.7})$$

we obtain¹

$$d\rho = 2a \frac{dv - du}{(u-v)^2} \quad (\text{B.8})$$

$$dz = 2a \frac{udv - vdu}{(u-v)^2}. \quad (\text{B.9})$$

Inserting du and dv in Eq. (B.6) we get

$$\begin{aligned} \frac{dv - du}{(v^2 + 1)^{\frac{3}{2}} - (u^2 + 1)^{\frac{3}{2}}} &= \frac{udv - vdu}{u(v^2 + 1)^{\frac{3}{2}} - v(u^2 + 1)^{\frac{3}{2}}} \\ (dv - du) \left[u(v^2 + 1)^{\frac{3}{2}} - v(u^2 + 1)^{\frac{3}{2}} \right] &= (udv - vdu) \left[(v^2 + 1)^{\frac{3}{2}} - (u^2 + 1)^{\frac{3}{2}} \right] \\ -vdu(u^2 + 1)^{\frac{3}{2}} - udu(v^2 + 1)^{\frac{3}{2}} &= -udv(u^2 + 1)^{\frac{3}{2}} - vdu(v^2 + 1)^{\frac{3}{2}} \\ (udv - vdu)(u^2 + 1)^{\frac{3}{2}} &= (udu - vdu)(v^2 + 1)^{\frac{3}{2}}. \end{aligned}$$

Thus, the variables u, v can be separated

$$\frac{du}{\sqrt{(u^2 + 1)^3}} = \frac{dv}{\sqrt{(v^2 + 1)^3}}. \quad (\text{B.10})$$

Integrating equation² (B.10), the result is

$$\frac{u}{\sqrt{u^2 + 1}} - \frac{v}{\sqrt{v^2 + 1}} = C \quad (\text{B.11})$$

with C as constant of integration. Substituting the original variables ρ and z into result (B.11) we get Eq. (3.38)

$$\frac{z_+}{\sqrt{z_+^2 + \rho^2}} - \frac{z_-}{\sqrt{z_-^2 + \rho^2}} = C. \quad (\text{B.12})$$

We are looking for solutions of $\cos \theta$ for $-1 \leq \cos \theta \leq 1$. Therefore, we assign $C = 1$ and obtain

$$\cos \theta = 1 - \frac{z_+}{\sqrt{z_+^2 + \rho^2}} + \frac{z_-}{\sqrt{z_-^2 + \rho^2}}. \quad (\text{B.13})$$

¹

$$dz = \frac{a}{(u-v)^2} [(du + dv)(u-v) - (u+v)(du - dv)] = 2a \frac{udv - vdu}{(u-v)^2}$$

²To integrate Eq. (B.10), we use the following identity

$$\frac{d}{du} \frac{u}{\sqrt{u^2 + 1}} = \frac{1}{(u^2 + 1)^{\frac{3}{2}}}.$$

Appendix C

Parallel transport and covariant derivative

We investigate a vector field C_μ along a curve $\mathcal{C}_{x'x}$ in space-time from x to x' . The curve is parametrized by a scalar s with

$$c^\mu(s), \quad s \in [0, 1], \quad \text{and} \quad c^\mu(0) = x^\mu, \quad c^\mu(1) = x'^\mu.$$

Now, we introduce a mapping $U(\mathcal{C}_{x'x}) \in \mathbf{SU}(n)$ between the vector spaces \mathcal{V}_x and $\mathcal{V}_{x'}$ at x and x'

$$U(\mathcal{C}_{x'x}) : \mathcal{V}_x \longrightarrow \mathcal{V}_{x'}.$$

The *parallel transporter* $U(\mathcal{C}_{x'x})$ defines the vector $U(\mathcal{C}_{x'x})C_\mu(x) \in \mathcal{V}_{x'}$, which is the parallel transported pendant of $C_\mu(x)$. $U(\mathcal{C})$ has to satisfy following conditions

- $U(0) = \mathbb{1}$, where 0 denominates a curve of length zero.
- $U(\mathcal{C}_2 \circ \mathcal{C}_1) = U(\mathcal{C}_2)U(\mathcal{C}_1)$ with composition of path \mathcal{C}_1 and \mathcal{C}_2 .
- $U(\mathcal{C}_{x'x}) = U^{-1}(\mathcal{C}_{xx'})$, where $\mathcal{C}_{xx'}$ is the reverse path of $\mathcal{C}_{x'x}$.

Under a local gauge transformation, like in Eq. (4.26), a parallel transporter transforms as

$$U(\mathcal{C}_{x'x}) \longrightarrow U'(\mathcal{C}_{x'x}) = \Lambda^{-1}(x'^\mu)U(\mathcal{C}_{x'x})\Lambda(x^\mu). \quad (\text{C.1})$$

Coordinate differences are meaningful only for vectors in the same vector space. Therefore, vectors at infinitesimal neighbouring points x'^μ and $x'^\mu = x^\mu + dx^\mu$ can only be compared by parallel transporting them to the same point. The *covariant differential* is defined by

$$DC_\mu \equiv U^{-1}(\mathcal{C}_{x+dx,x})C_\mu(x+dx) - C_\mu(x). \quad (\text{C.2})$$

For an infinitesimal distance dx^μ the parallel transporter $U(\mathcal{C}_{x+dx,x})$ can be expanded in a Taylor series

$$U(\mathcal{C}_{x+dx,x}) = \mathbb{1}_n + iA_\mu dx^\mu + \mathcal{O}(dx^\mu)^2 \quad (\text{C.3})$$

with A_μ being an element of the $\mathfrak{su}(n)$ Lie-algebra¹. By neglecting orders $\mathcal{O}(dx^\mu)^2$ and higher we obtain for the covariant differential

$$\begin{aligned} DC_\mu &= [\mathbb{1}_n + iA_\nu dx^\nu + \mathcal{O}(dx^\mu)^2]^{-1} C_\mu(x+dx) - C_\mu(x) \\ &= [\mathbb{1}_n - iA_\nu dx^\nu] [C_\mu(x) + \partial_\nu C_\mu(x) dx^\nu + \mathcal{O}(dx^\nu)^2] - C_\mu(x) \\ &= C_\mu(x) + \partial_\nu C_\mu(x) dx^\nu - iA_\nu dx^\nu C_\mu(x) + \mathcal{O}(dx^\mu)^2 - C_\mu(x) \\ &= \underbrace{[\partial_\nu - iA_\nu]}_{D_\nu} C_\mu(x) dx^\nu = D_\nu C_\mu(x) dx^\nu, \end{aligned} \quad (\text{C.4})$$

where $D_\nu = \partial_\nu - iA_\nu$ is the *covariant derivative*. The functions A_ν in Eq. (C.3) are denoted *gauge field*. Based on the gauge transformation law of parallel transporters (C.1) and using the Taylor expansion of $\Lambda^{-1}(x+dx)$

$$\Lambda^{-1}(x+dx) = \Lambda^{-1}(x) + \partial_\mu \Lambda^{-1}(x) dx^\mu + \mathcal{O}(dx^\mu)^2$$

we are able to write

$$\begin{aligned} \mathbb{1}_n + iA'_\mu dx^\mu &= \Lambda^{-1}(x^\mu) [\mathbb{1}_n + iA_\mu dx^\mu] \Lambda(x^\mu) \\ &= [\Lambda^{-1}(x^\nu) + \partial_\mu \Lambda^{-1}(x^\nu) dx^\mu] [\mathbb{1}_n + iA_\mu dx^\mu] \Lambda(x^\nu) \\ &= \mathbb{1}_n + \partial_\mu \Lambda^{-1}(x^\nu) dx^\mu \Lambda(x^\nu) + i\Lambda^{-1}(x^\nu) A_\mu \Lambda(x^\nu) dx^\mu + \mathcal{O}(dx^\mu)^2. \end{aligned}$$

Comparing the coefficients follows the transformation law of the gauge field

$$\begin{aligned} A'_\mu &= \Lambda^{-1}(x^\nu) A_\mu \Lambda(x^\nu) + \frac{1}{i} \partial_\mu \Lambda^{-1}(x^\nu) \Lambda(x^\nu) \\ &= \Lambda^{-1}(x^\nu) [A_\mu + i\partial_\mu] \Lambda(x^\nu), \end{aligned} \quad (\text{C.5})$$

where the identity

$$(\partial_\mu \Lambda^{-1}) \Lambda = \underbrace{\partial_\mu (\Lambda^{-1} \Lambda)}_{=0} - \Lambda^{-1} \partial_\mu \Lambda = -\Lambda^{-1} \partial_\mu \Lambda$$

is used. Therefore, covariant derivatives transform like vectors and like gradients of a scalar fields² $\phi(x)$, that is

$$D'_\nu \phi'(x') = \Lambda^{-1}(x) D_\nu \phi(x). \quad (\text{C.6})$$

¹Reminder: The definition of Lie-algebra $\mathfrak{su}(n)$ is found in section 2.4

²The transformation of a scalar field obeys $\phi'(x') = \phi(x)$. A scalar never changes its value under base transformations.

Applying commutation relation to two covariant derivatives, Eq. (C.4) the result is nothing else but a definition of the curvature tensor $R_{\mu\nu\sigma}^\lambda$ in Riemann differential geometry and is likewise computed in our *model of topological fermions*³. The field strength tensor $F_{\mu\nu}$, being proportional to curvature tensor $R_{\mu\nu KM}$, see Eq. (2.91) can be written exactly in the same manner

$$iR_{\mu\nu} = [D_\mu, D_\nu] = -i(\partial_\mu A_\nu - \partial_\nu A_\mu) - [A_\mu, A_\nu]. \quad (\text{C.7})$$

The above result, interpreted in a geometrical manner can be considered as parallel transport around an infinitesimal parallelogram spanned by dx^μ and dy^ν , see Fig. 4.2a on page 49. The corresponding parallel transporter is given by

$$U(\mathcal{C}_{x,x}) = \mathbb{1}_n - iR_{\mu\nu}dx^\mu dy^\nu. \quad (\text{C.8})$$

Therefore, the curvature tensor transforms under a local gauge transformation as

$$R_{\mu\nu} \longrightarrow R'_{\mu\nu} = \Lambda^{-1}(x) R_{\mu\nu} \Lambda(x). \quad (\text{C.9})$$

³Compare section 2.5.4, notably Eq. (2.88).

Appendix D

Command-line options of program sol

Program execution can be done on command line with

```
$ ./sol [options] [filename] ↵
```

option	effect
-1	Indicates a monopole calculation, by using the appropriate subprocedures, a soliton configuration at the origin is supposed. This option is mutual exclusive with -2 .
-2	Indicates a dipole configuration. Two monopole solitons are placed on the 3-axis at a distance $\pm d/2$ from the origin. This option is mutual exclusive with -1 .
-y	Before starting the energy-minimizing-routines, there is an enquiry about. This question is essential to shell scripts. This option is mutual exclusive with -n .
-n	This option has opposite meaning of the previous parameter and is mutual exclusive with -y .
-R n_r	This parameter defines the number $n_r \in \mathbb{N}$ of points of the lattice in r -direction. In general, it is combined with the corresponding parameters for z .
-Z n_z	This parameter defines the number $n_z \in \mathbb{N}$ of points of the lattice in z -direction. However, the origin is defined at $n_z/2$. Usually specified together with -R n_r on the command line.
-r \bar{r}_0	Specifies the soliton radius $\bar{r}_0 \in \mathbb{N}$ in lattice units a .
-f f_r	Denotes the region with fixed soliton field by the radius f_r in lattice units a . Inside the radius f_r the field is not minimized, avoiding lattice artifacts.

-d d	Declares the distance of both soliton centers on the 3-axis. That means, soliton centers are settled at a distance $\pm d/2$ from the origin.
-I i	Selects the type of integration procedure by $i = 1, 2, 3, 4$. With $i = 1$ or 2 , a Simpson rule of numerical integration [18] is chosen, just executed for different variable types (<code>int</code>) and (<code>double</code>), respectively. With $i = 3$ or 4 , a simple sum is used for integration, hence, for same types of variables (<code>int</code>) and (<code>double</code>). The default option is the value $i = 4$.
-w	Indicates to compute the Wilson action. Default value is to go without.
-l	The output is formatted as a latex line for further processing.
-s	The lattice computations are done without tiles until 500 iterations. Without this option the lattice is divided in overlapping tiles, calculating more but smaller parts and resulting in more accurate minimizations.
-D	Debug option, interim results are displayed.

Table D.1: Listing of all options, used by lattice simulation program: `sol`. Default values of passing parameters can be found in `definitions.h`.

Bibliography

- [1] http://en.wikipedia.org/wiki/Democritus#Atomic_hypothesis, Philosophy and science of Democritus
- [2] http://en.wikipedia.org/wiki/Atomic_theory
- [3] <http://plato.stanford.edu/archives/fall2008/entries/atomism-modern/>
- [4] Geiger, H., *On the Scattering of α -Particles by Matter*, Proceedings of the Royal Society of London A 81 (546): 174–177. (1908)
- [5] Cottingham, W. N., Greenwood, D. A., *An introduction to the standard model of particle physics*, second edition, University of Bristol, Cambridge Press (2007)
- [6] Perring, J. K., Skyrme, T. H. R., *A model unified field equation*, Nucl. Phys. 31, 550-555, (1962)
- [7] Remoissenet, M., *Waves called solitons* third edition, Springer Verlag Berlin Heidelberg New York, (1999)
- [8] Abarbanel, H. D. I., Rabinovich, M. I., Sushchik, M. M., *Introduction to nonlinear dynamics for physicists* Department of Physics and Institute for Nonlinear Science, University of California, San Diego (1993)
- [9] https://en.wikipedia.org/wiki/Orthogonal_group
- [10] Böhm, M., *Lie-Gruppen und Lie-Algebren in der Physik*, Universität Gießen, Springer Verlag (2011)
- [11] Puri, R. R., *Mathematical Methods of Quantum Optics*, Berlin, Springer (2001)
- [12] https://en.wikipedia.org/wiki/Special_unitary_group
- [13] Jech, M., *Die Hopf-Zahl in einer $SU(2)$ -Feldtheorie* Diplomarbeit, TU Wien (2014)
- [14] Höllwieser, R., *Punktförmige und ausgedehnte Monopole am Raum-Zeit-Gitter*, Diplomarbeit, TU Wien (2006)

- [15] Faber, M., *Solitonen, Differentialgeometrie und Topologie*, Scriptorum, TU Wien
- [16] Wabnig, J., *Interaction in the Model of Topological Fermions*, Diplomarbeit, TU Wien (2001)
- [17] Resch, J., *Numerische Analyse an Dipolkonfigurationen im Model topologischer Fermionen*, Diplomarbeit, TU Wien (2010)
- [18] Press, W. H., Teukolsky, S., Vetterling, W. T., Flannery, B. P., *Numerical Recipes in C*, The art of scientific computing, second edition, Cambridge University Press (1992)
- [19] Montvay, I., Münster, G., *Quantum fields on a lattice*, Cambridge University Press (1994)
- [20] Wilson, K. G., *Confinement of quarks*, Phys. Rev. D10, p2445, (1974)
- [21] <http://physics.nist.gov/cgi-bin/cuu/Value?alph>
- [22] Jackson, J. D., *Classical Electrodynamics*, second edition, University of California, Berkeley, John Wiley & Sons, New York (1975)
- [23] Vilasi, G., *Hamiltonian Dynamics*, University of Salerno, World Scientific Publishing Co. Pte. Ltd. (2001)